BIOPROBES 76

JOURNAL OF CELL BIOLOGY APPLICATIONS NOVEMBER 2017

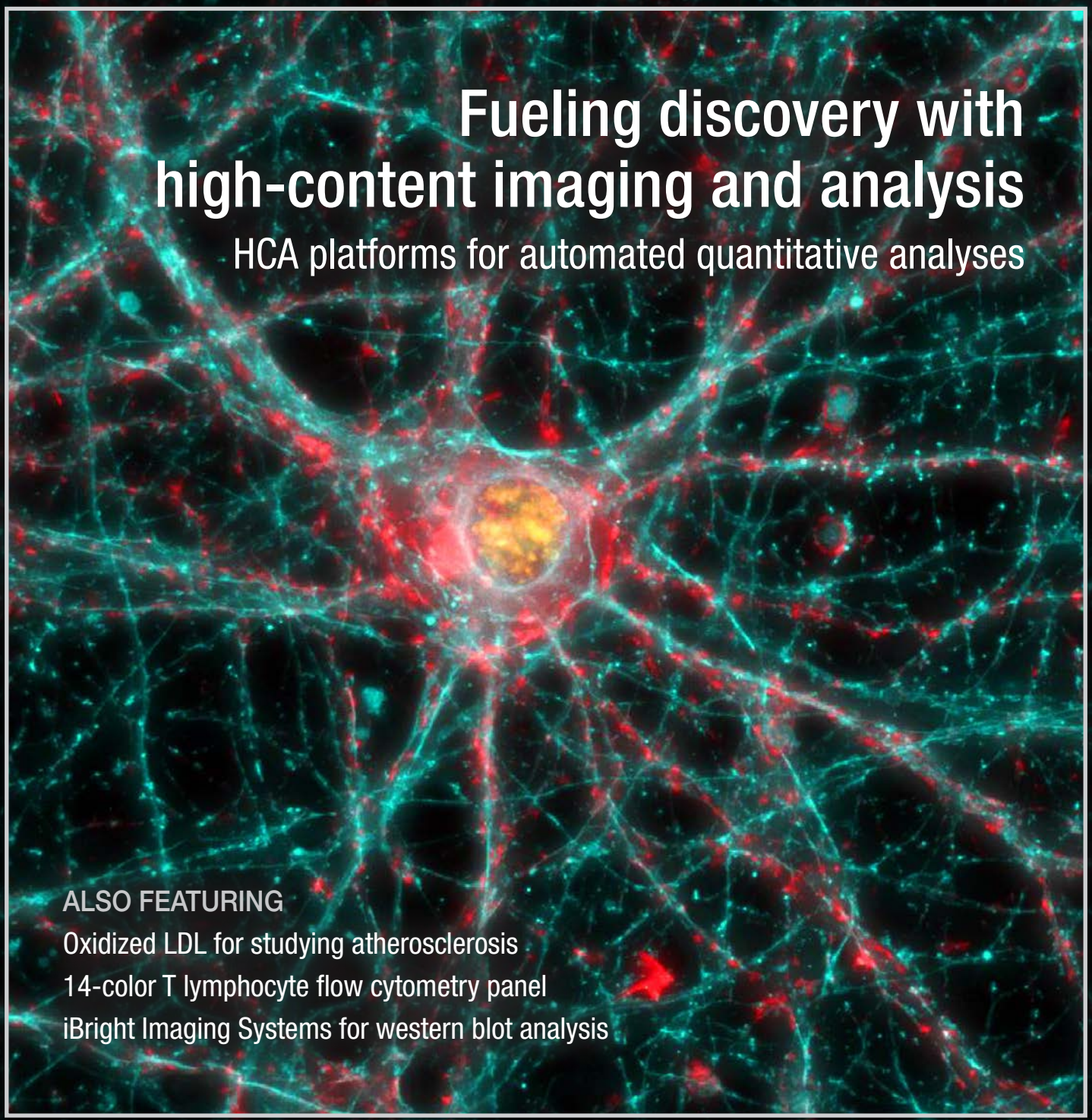

Fueling discovery with high-content imaging and analysis

HCA platforms for automated quantitative analyses

ALSO FEATURING

Oxidized LDL for studying atherosclerosis

14-color T lymphocyte flow cytometry panel

iBright Imaging Systems for western blot analysis

invitrogen
by Thermo Fisher Scientific

invitrogen

Bound to work

Antibodies

We're testing Invitrogen antibodies to meet the newest specificity standards

We're committed to superior antibody performance. That's why we're rigorously testing our Invitrogen™ antibodies using a two-part approach for advanced verification—so you can be confident your Invitrogen antibody will bind to the correct target in your intended application.

Learn about our two-part approach to antibody testing at
thermofisher.com/antibodyvalidation

ThermoFisher SCIENTIFIC

BioProbes 76

invitrogen

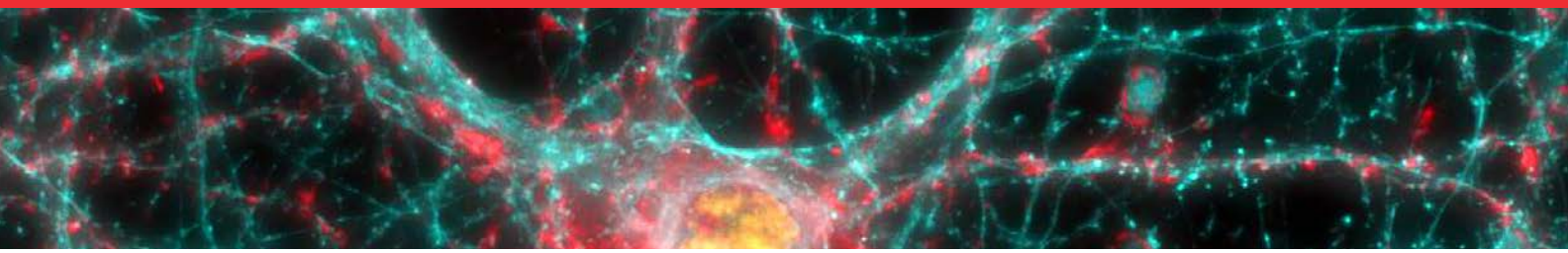

thermofisher.com/bioprobes • November 2017

ONLINE AND ON THE MOVE

2 | Molecular Probes School of Fluorescence, Immune Cell Guide, on-demand webinars, and more

JUST RELEASED

4 | Our newest cellular analysis products and technologies

FLUORESCENCE IMAGING APPLICATIONS

6 | Fueling discovery with high-content imaging and analysis
Thermo Scientific HCA platforms for automated, quantitative analyses

10 | Appetite for destruction
Studying macroautophagy with Premo fluorescent protein–based sensors

13 | Effectively monitor antibody internalization and trafficking
Improved labeling tools for antibody–drug conjugate screening and characterization

16 | Investigate atherosclerosis with modified low-density lipoproteins
Fluorescently labeled oxidized LDLs and acetylated LDLs

19 | Double vision: Simultaneous visualization of protein and RNA targets
ViewRNA Cell Plus Assay for antibody labeling and in situ *hybridization in individual cells*

22 | Maximize survival of neurons derived from primary and stem cells
Introducing the Gibco B-27 Plus Neuronal Culture System

RESEARCH WITH ANTIBODIES

24 | T lymphocyte immunophenotyping
14-color flow cytometry panel featuring Super Bright antibody conjugates

26 | Boost your stem cell antibody arsenal
Monoclonal antibodies for studying human pluripotent stem cells

28 | The new generation of target-specific protein quantitation
Introducing ProQuantum high-sensitivity immunoassays

TOOLS FOR PROTEIN ANALYSIS

30 | Stunningly easy western blot imaging
Introducing the iBright CL1000 and iBright FL1000 Imaging Systems

32 | Optimize protein integrity and yields during workflows
Broad-spectrum protease and phosphatase inhibitor tablets

BEHIND THE BENCH BLOG

33 | Discussing the "Maximum Event Rate" of your flow cytometer

JOURNAL CLUB

35 | Time-resolved analysis of proteome dynamics by TMT-SILAC hyperplexing

36 | An evaluation of dyes for tracking cell proliferation by flow and image cytometry

BioProbes Journal, available in print and online at **thermofisher.com/bioprobes**, is dedicated to providing researchers with the very latest information about cell biology products and their applications. For a complete list of our products, along with extensive descriptions and literature references, please see our website.

ThermoFisher SCIENTIFIC

Molecular Probes School of Fluorescence—Flow Cytometry Basics Module

Do you ever wonder how a flow cytometer works? Need to understand the optical setup of a flow cytometer? Now you can find answers to these questions and more in the Invitrogen™ Molecular Probes™ School of Fluorescence—Flow Cytometry Basics module, available online. The Flow Cytometry Basics module is designed to help you understand the fundamentals. This online content covers the three main components of a flow cytometer: fluidics, optics, and electronics, and was written by the bench scientists who created the *Molecular Probes Handbook*. Learn more at **thermofisher.com/mpsf-flow**.

Antibody reproducibility standards: A panel discussion with key scientific leaders

Antibody reproducibility and antibody validation* are two significant challenges facing scientific researchers today. Thermo Fisher Scientific recently hosted a roundtable panel discussion in which members from the International Working Group on Antibody Validation (IWGAV), others from the research community, and key Thermo Fisher Scientific personnel participated in a dialogue about antibody validation standards and practices. These researchers addressed the antibody crisis with recommendations to develop standards that ensure proper characterization and consistency for antibodies in the laboratory. Now you can watch the video and hear the discussion at **thermofisher.com/antibodyvalidation**. While there, you can learn more about how Thermo Fisher Scientific is validating antibodies for both functional application and specificity verification.

*The use or any variation of the word "validation" refers only to research use antibodies that were subject to functional testing to confirm that the antibody can be used with the research techniques indicated. It does not ensure that the product(s) was validated for clinical or diagnostic uses.

Announcing the winners of the Thermo Fisher Scientific Antibody Scholarship Program

Over the past several years, the Thermo Fisher Scientific Antibody Scholarship Program has awarded $400,000 in scholarship funds to 60 deserving undergraduate and graduate students in the field of biological research. The goal of this program is to ensure well-educated students are prepared for future scientific research, teaching, and technological developmental opportunities. We receive applications from students across the United States who show a passion for science and learning and have a wide variety of interests and achievements in science. Check our website to read more about the scholarship, the application requirements, and the winners at **thermofisher.com/antibodyscholarship**. The Fall 2017 scholarship winners are:

- Nathaniel Deimler, Nova Southeastern University
- Ana Enriquez, Emory University
- Micheal Munson, Baylor University
- Kritika Singh, Northeastern University
- Emily Xu, Yale University
- Joshua Yang, Johns Hopkins University

Download the Immune Cell Guide

Download the newly updated Invitrogen™ Immune Cell Guide, which includes markers for B cells, T cells, dendritic cells, granulocytes, macrophages, and stem cells, just to name a few. Human and mouse antigens and cluster of differentiation (CD) and non-CD antigens are listed in this useful resource. Visit the Antibodies for Flow Cytometry landing page to download a digital copy of the Immune Cell Guide today at **thermofisher.com/flowantibodies**.

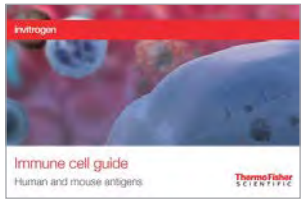

Protein Assay Technical Handbook now available

The 60-page Protein Assay Technical Handbook from Thermo Fisher Scientific provides strategies to help you optimize your protein quantitation results. Select your assay method of choice based on assay time, sensitivity, compatibility, standard curve linearity, and protein-to-protein variation. Learn about tools and resources to help choose the right quantitation assays for your research, ensuring more accurate downstream results. Download a digital copy of the handbook at **thermofisher.com/protein-assay-handbook**.

On-demand educational webinars

The Protein and Cell Analysis Education site is a free-access virtual learning environment that showcases educational webinars focused on protein and cell analysis and on antibodies and immunoassays. These webinars cover the newest applications and techniques related to fluorescence imaging, high-content analysis, flow cytometry, western blot detection, gel electrophoresis, mass spectrometry, and more. Now you can easily access our on-demand webinars and see what new webinars are coming up at **thermofisher.com/pcawebinars**.

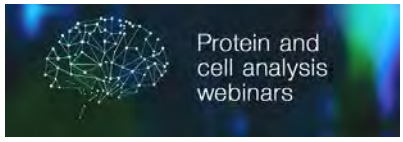

Invitrogen secondary antibodies: Winner of the 2017 CiteAb award

At Thermo Fisher Scientific, we are proud to receive the 2017 CiteAb award for our Invitrogen™ secondary antibodies. In awarding this distinction, CiteAb recognized Thermo Fisher Scientific as the most successful company at providing secondary antibodies, based on the number of citations of Invitrogen secondary antibodies in 2016.

Thermo Fisher Scientific offers a comprehensive portfolio of conjugated and unconjugated secondary antibodies for fluorescent, colorimetric, and chemiluminescent detection of primary antibodies in a wide range of applications, including cell imaging, flow cytometry, and western blotting. Browse our secondary antibody selection guide and find out more about choosing the right fluorescent secondary antibody at **thermofisher.com/antibodies**.

Using CFSE? Have a UV laser? Try our UV-excitable CellTrace Blue cell proliferation reagent

The Invitrogen™ CellTrace™ Blue Cell Proliferation Kit is an alternative to CFSE for tracing multiple generations by dye dilution using flow cytometry. The CellTrace Blue cell proliferation reagent can be used in the same applications as CFSE and other CellTrace reagents; however, it was specifically designed for excitation by a UV laser (355 nm or 375 nm). The CellTrace Blue reagent can easily be multiplexed with reagents and antibodies that are excited by other commonly used lasers. With the development of the CellTrace Blue dye, we now offer a full portfolio of CellTrace cell proliferation reagents, including the widely used Invitrogen™ CellTrace™ Violet reagent; see page 36 for the Journal Club article "An evaluation of spectrally distinct succinimidyl ester dyes for tracking cell proliferation by flow and image cytometry." From UV to red laser excitation, we have a CellTrace reagent for your existing flow panels; see the selection guide at **thermofisher.com/celltrace**.

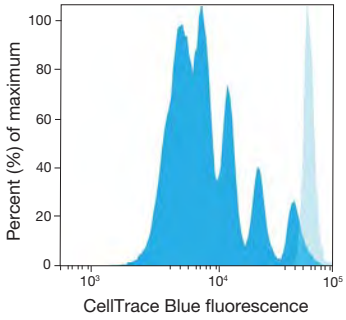

Tracking cell division using CellTrace Blue reagent. Human peripheral blood mononuclear cells (PBMCs) were stained with 10 µM Invitrogen™ CellTrace™ Blue reagent (Cat. No. C34574). The blue peaks represent successive generations of cells stimulated with Gibco™ Dynabeads™ Human T-Expander CD3/CD28 (Cat. No. 11141D) and cultured for 5 days. The light blue peak represents cells that were cultured with no stimulus. Data were collected on a BD™ LSR II Flow Cytometer with 355 nm excitation and a 450/50 nm bandpass emission filter.

Super Bright antibody conjugates: Superb alternatives to Brilliant Violet conjugates for flow cytometry

Invitrogen™ eBioscience™ Super Bright antibody conjugates are now available in an even greater variety of markers, clones, and formats. With over 400 products covering more than 100 different clones (including both human and mouse antigens), you have even more options for your violet laser. Discriminate dim cell populations more easily using Super Bright 436, Super Bright 600, Super Bright 645, or Super Bright 702 antibody conjugates for flow cytometry. As compared with Brilliant Violet™ conjugates, the Super Bright conjugates display similar or better brightness and some have been shown to require less compensation. Discover your options and find a Super Bright antibody conjugate that fits your flow cytometry panel at **thermofisher.com/superbright**.

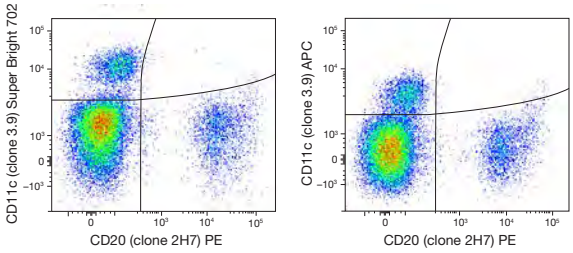

Better resolution achieved with Super Bright antibody conjugates vs. APC antibody conjugates. Human peripheral blood mononuclear cells (PBMCs) were stained with PE anti–human CD20 antibody (Cat. No. 12-0209-42) and anti–human CD11c antibody conjugated either to Super Bright 702 dye (left, Cat. No. 67-0116-42) or to APC (right, Cat. No. 17-0116-42). CD11c+ cells stained with Super Bright antibodies demonstrate better resolution than those stained with APC antibodies.

No-Weigh packaging now available for protein modification reagents

Thermo Scientific™ No-Weigh™ products are specialty protein modification reagents provided in a pre-aliquoted format. The pre-weighed packaging prevents contamination and loss of reagent reactivity over time by eliminating the repetitive opening and closing of the vial. It also eliminates the hassle of weighing small amounts of reagent; a ready-to-use solution can be made quickly and conveniently. The No-Weigh packaging format is available in convenient fill sizes using PCR strip tubes or easy-to-handle screw cap vials for popular protein reagents, including reducing agents, crosslinkers, and PEG- and biotin-labeling products. Find out more at **thermofisher.com/no-weigh**.

No-Weigh packaging. Thermo Scientific™ No-Weigh™ packaging is now available for widely used protein modification reagents such as reducing agents, crosslinkers, and labeling products. An example of the pre-aliquoted screw cap vials is shown here.

More Alexa Fluor dye–conjugated organelle-specific antibodies

Thermo Fisher Scientific has launched additional organelle-specific fluorescent antibodies for use in colocalization and other immunofluorescent experiments. We now offer over 30 different organelle-specific antibodies preconjugated to highly fluorescent Invitrogen™ Alexa Fluor™ dyes. These organelle-specific antibodies are high-affinity monoclonal and polyclonal antibodies that recognize cellular targets normally restricted to specific organelles, including mitochondria, lysosomes, endoplasmic reticulum, nucleus, nucleolus, and more. No secondary detection reagents are required so multiplex experiments are greatly simplified. See all of the organelle-specific antibodies at **thermofisher.com/organelleabs**.

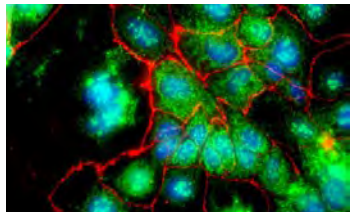

Multiplexed staining of cell junctions, mitochondria, and nucleoli. Fixed, permeabilized, and blocked Caco-2 cells were labeled with Invitrogen™ Alexa Fluor™ 647 anti–ZO-1 (red, Cat. No. MA3-39100-A647), Alexa Fluor™ 488 anti–ATP synthase β (orange, Cat. No. MA1-930-A488), Alexa Fluor™ 488 anti-nucleophosmin (green, Cat. No. MA3-25200-A488), and Hoechst™ 33342 (blue, Cat. No. 62249). Cells were imaged on an Invitrogen™ EVOS™ FL Auto Imaging System at 60x magnification.

Now available: ProLong Glass Antifade Mountant

The Invitrogen™ ProLong™ Glass Hard-Set Antifade Mountant is a ready-to-use mountant with a high refractive index (1.52 after curing) that results in up to 75% more axial resolution and superior lateral resolution when compared with low refractive index mountants. This mountant delivers excellent signal-to-background ratios and photobleaching protection for organic fluorophores and fluorescent proteins, making it ideal for producing sharp, bright, high-quality images of any cell or tissue sample up to 100 µm in thickness with almost any fluorescence microscope. Find out more at **thermofisher.com/antifades**.

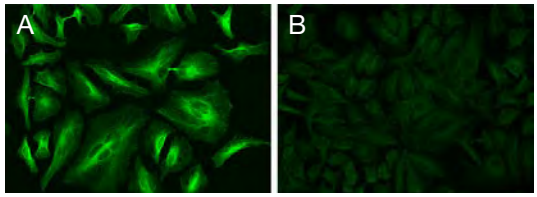

Photobleaching protection by ProLong Glass mountant. HeLa cells were labeled with anti-tubulin antibody, detected with fluorescein (FITC) secondary antibody, and mounted in **(A)** Invitrogen™ ProLong™ Glass mountant (Cat. No. P36980) or **(B)** 50% glycerol in PBS. The samples were then illuminated for 60 sec using a 100 W Hg-arc lamp and imaged using a 20x air objective and a 12-bit monochrome camera.

Pierce Rapid Gold BCA Protein Assay provides highly accurate results in 5 minutes

The Thermo Scientific™ Pierce™ Rapid Gold BCA Protein Assay Kit is a high-precision, two-component, detergent-compatible assay for measuring total protein concentration with copper-chelating technology (using absorbance at 480 nm). This assay provides the same accuracy and detergent compatibility as the traditional BCA assay but in only 5 minutes and with a room-temperature incubation that eliminates the need to expose samples to elevated temperatures. Learn more about the Pierce Rapid Gold BCA assay, which can be adapted for use with microplate readers and spectrophotometers, at **thermofisher.com/bca-assays**.

Product	Quantity	Cat. No.
Pierce Rapid Gold BCA Protein Assay Kit	20 mL	A53227
	250 mL	A53226
	500 mL	A53225

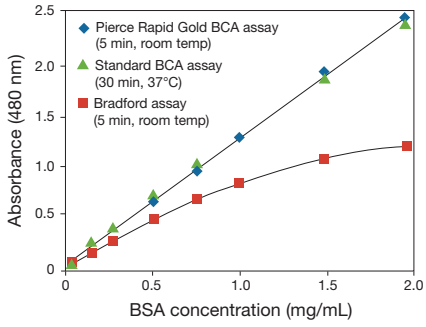

The Pierce Rapid Gold BCA Protein Assay provides the accuracy of the BCA assay with the speed of the Bradford assay. Standard curves for the Thermo Scientific™ Pierce™ Rapid Gold BCA Protein Assay, Pierce™ BCA Protein Assay, and Bio-Rad™ Bradford Protein Assay were produced using purified BSA in 0.9% saline. All assays were conducted according to the manufacturer's protocol in a microplate format.

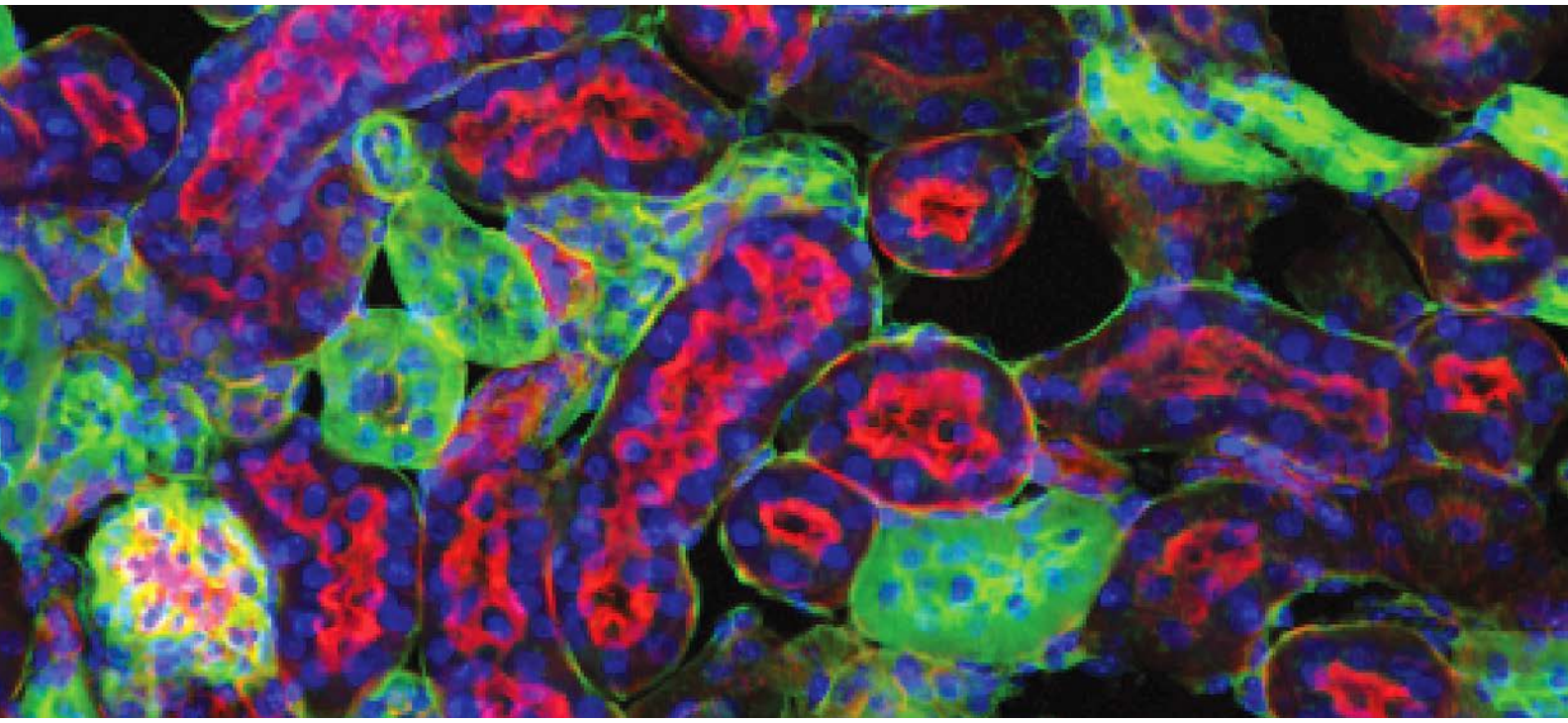

Fueling discovery with high-content imaging and analysis

Thermo Scientific HCA platforms for automated, quantitative analyses.

A wealth of information about a physiological process or pathological condition can be collected by monitoring the localization and abundance of specific proteins using fluorescence imaging (Figure 1). The use of fluorescence imaging in conjunction with biosensors that incorporate synthetic organic dyes or fluorescent proteins allows researchers to visualize protein and organelle functioning during cellular processes in real time. However, quantifying these essential processes through the capture and analysis of fluorescence imagery is both time consuming and laborious. With the advent of high-content analysis platforms that automate image capture and data analysis, these obstacles have been removed, affording researchers both the sample sizes and precise quantitation tools required for truly robust and reproducible research.

Figure 1. Confocal image of a fluorescently stained mouse kidney. See Figure 2 caption for experimental details.

Thermo Scientific HCA platforms and software

Among the most cited in scientific articles, high-content analysis (HCA) instruments from Thermo Fisher Scientific are the go-to choice for researchers requiring the resolution of microscopy with the statistical power inherent in a highly quantitative analysis of a large number of cells. These instruments include the Thermo Scientific™ ArrayScan™ High-Content Platforms, the Thermo Scientific™ CellInsight™ CX5 High-Content Screening (HCS) Platform, and the recently introduced Thermo Scientific™ CellInsight™ CX7 High-Content Analysis (HCA) Platform. The CellInsight CX7 HCA Platform provides an integrated benchtop instrument that interrogates multiple sample types with a wide range of techniques, taking advantage of next-level image acquisition and analysis software (Figure 2).

In the first half of this year, our HCA platforms have been used in nearly one hundred peer-reviewed publications. Many of these high-content imaging and analysis studies take advantage of the Thermo Scientific™ HCS Studio™ software provided with our HCA instruments (Figures 2 and 3). This intuitive, icon-driven tool helps to manage the experimental design and workflow, starting with plate maps and protocol setup, all the way through image acquisition and data analysis. Once images are acquired, users can leverage the software's suite of available bioapplications, purpose-built for specific biological areas such as proliferation, translocation, neurite outgrowth, and autophagy. The following sections contain short summaries of key publications in which Thermo Scientific HCA platforms and software have been used to make critical discoveries across multiple research areas.

Investigating infectious diseases

Love and coworkers recently published work on the infection of human intestinal epithelial cells by the parasite *Cryptosporidium parvum*, which causes a life-threatening diarrheal disease in children [1]. Using the CellInsight CX5 High-Content Screening (HCS) Platform, Love et al. screened a library of existing FDA-approved molecules in search of inhibitors of *Cryptosporidium* spp. proliferation. This research highlights the use of automated image acquisition and analysis to detect events within a cell that can lead to potential novel therapeutic applications, in this case the identification of the drug clofazimine as an inhibitor of *C. parvum* infection. →

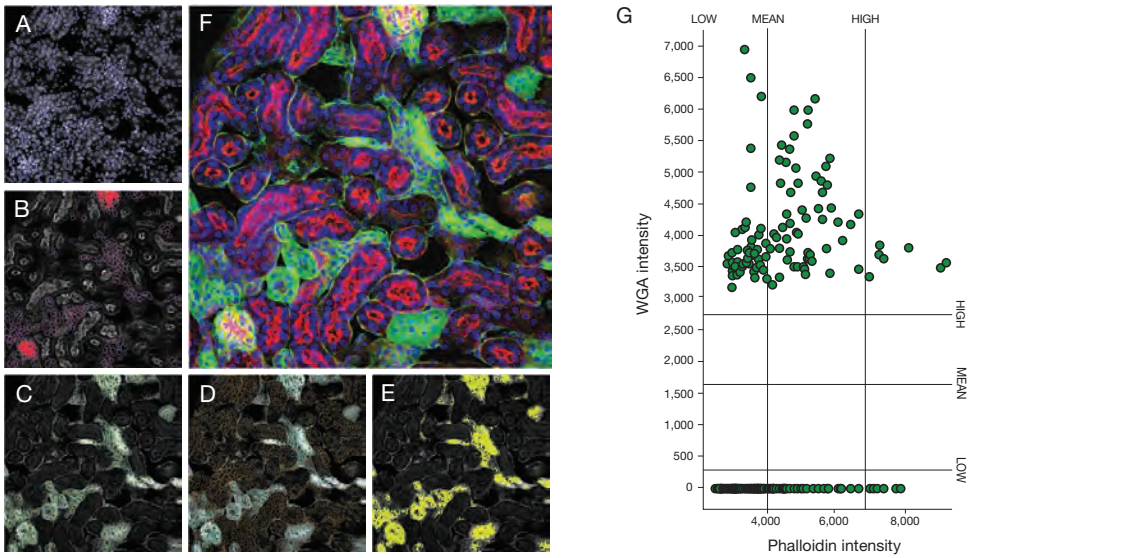

Figure 2. Confocal image analysis of a fluorescently stained mouse kidney. A 16 µm cryostat section of mouse kidney was stained with Invitrogen™ Alexa Fluor™ 488 Wheat Germ Agglutinin (WGA) (green, Cat. No. W11261), Invitrogen™ Alexa Fluor™ 568 Phalloidin (red, Cat. No. A12380), and DAPI nucleic acid stain (blue, Cat. No. D1306) and imaged on the Thermo Scientific™ CellInsight™ CX7 High-Content Analysis Platform using laser autofocus and confocal acquisition at 20x magnification. Thermo Scientific™ HCS Studio™ Cell Analysis Software was used for analysis: **(A)** nuclear identification and segmentation (blue); **(B)** phalloidin detection in WGA+ cells (red); **(C)** WGA+ cell selection (green); **(D)** WGA mask modification (green); **(E)** spot detection for quantifying WGA signal; **(F)** composite confocal image. **(G)** Scatter plot shows relative labeling intensity of the WGA vs. phalloidin conjugates in order to characterize phenotypes using intensity cutoffs.

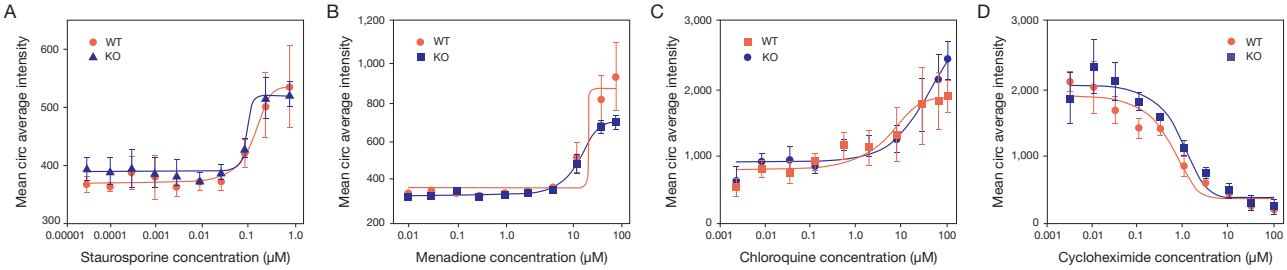

Figure 3. Rapid analysis of various cell health parameters using a high-content analysis (HCA) platform. Wild-type (WT) and CRISPR-edited (functional knockout or KO) HAP1 cells were analyzed using the Thermo Scientific™ CellInsight™ CX5 High-Content Screening Platform for **(A)** apoptosis, using Invitrogen™ CellEvent™ Caspase-3/7 Green ReadyProbes™ Reagent (Cat. No. R37111), **(B)** oxidative stress, using Invitrogen™ CellROX™ Green Reagent (Cat. No. C10444), **(C)** protein degradation, with the Invitrogen™ Click-iT™ HPG Alexa Fluor™ 488 Protein Synthesis Assay Kit (Cat. No. C10428), and **(D)** protein synthesis, using the Invitrogen™ Click-iT™ Plus OPP Alexa Fluor™ 488 Protein Synthesis Assay Kit (Cat. No. C10456). Thermo Scientific™ HCS Studio™ Cell Analysis Software was used for nuclear segmentation and fluorescence analysis (mean circ average intensity).

Assaying cell function and oxidative stress

High-content imaging and analysis can also be applied to the study of cell–cell interactions and more comprehensive tissue functions. Using the CellInsight CX5 High-Content Screening Platform, Summermatter and colleagues investigated the role of metallothioneins in regulating skeletal muscle mass [2]. Metallothioneins, a family of cysteine-rich metal-binding proteins, are involved in zinc storage and transport and have been implicated in muscle atrophy. Automated image capture of stained myofibers and subsequent analysis of their width showed that myofiber width increases following siRNA-mediated knockdown of metallothioneins, suggesting a new strategy for increasing muscle mass and strength.

Zhang et al. employed the ArrayScan VTI HCS Reader to study a different muscle cell type—cardiomyocytes. These authors demonstrated that, in neonatal mouse cardiomyocytes, mitochondria are the main source of the reactive oxygen species (ROS) generated following β-adrenergic receptor stimulation [3]. They further characterized the properties of these ROS bursts using the fluorogenic probes dihydroethidium and Invitrogen™ MitoSOX™ Red Mitochondrial Superoxide Indicator to show that two discrete pathways regulate the temporal profile of ROS generation. Faster mitochondrial ROS bursts are controlled by the cAMP/PKA pathway, whereas slower mitochondrial ROS production is regulated by the β-arrestin1 pathway.

Another important regulator of oxidative stress is the Nrf2 pathway, which was investigated by Pistollato and coworkers using the ArrayScan XTI High-Content Platform. These researchers measured the nuclear translocation of Nrf2 in response to rotenone treatment of neural stem cells derived from human induced pluripotent stem cells (iPSCs) [4]. They showed that Nrf2 translocation increases during differentiation and is associated with cytotoxicity. Using the neurite outgrowth bioapplication built into the HCS Studio software, they also found that Nrf2 activity was correlated with neurite retraction.

Studying neuronal development and disease

Neurite outgrowth is a key step in neuronal development. Once a critical cell mass is reached, a neural progenitor cell line derived from cortical neuroepithelium can extend neurites and form synaptic connections. Hill et al. studied how mutations in the transcription factor gene *TCF4* affect human cortical cell progenitor proliferation using the Thermo Scientific™ CellInsight™ NXT High-Content Screening Platform [5], and discuss the implications for cognitive deficits found in individuals with Pitt-Hopkins syndrome.

Lorenz et al. also characterized the cellular phenotype arising from gene mutations, in this case in the mitochondrial gene *MT-ATP6* [6]. *MT-ATP6* mutations have been shown to be associated with several neurological diseases, including Leigh syndrome, retinitis pigmentosa, and episodic paralysis with spinal neuropathy. These researchers produced neural progenitor cells from patient-derived iPSCs carrying mutations in the *MT-ATP6* gene, and showed that these cells exhibited abnormal mitochondrial membrane potential using the ArrayScan XTI Infinity High-Content Platform. They then performed a phenotypic screen of existing FDA-approved drugs using mitochondrial membrane potential as a phenotype, and found that one compound, avanafil, was able to alleviate the phenotype in mutation-carrying cells.

Table 1. Which HCA system is right for you?

	Compact screening system to scale up your throughput	Integrated performance modes for screening and analysis	Modular solutions to address specialized applications
	 CellInsight CX5 Platform	 CellInsight CX7 Platform	 ArrayScan Systems
Illumination	5 channels	7 channels	7 channels
Camera	Photometrics X1		
Widefield	5 channels	7 channels	7 channels
Brightfield	White	White + 4 colors	White (optional)
Confocal	NA	7 channels	7 channels (optional)
Objectives	1-position turret 2x to 20x	3-position turret 2x to 40x	4-position turret 1.25x to 63x
Focus	Software	Laser and software	Laser and software
Live cell	NA	NA	Live cell (optional)
Software	HCS Studio Cell Analysis Client Software		
Thermo Fisher Cloud	Save files to Cloud through computer		
Database	Store Image and Database Management Software (optional)		

Mitochondrial and lysosomal dysfunctions often coexist in neuronal diseases. Using primary neurons, Jinn and colleagues produced knockout mutations in *TMEM175*, a known risk-factor gene for Parkinson's disease [7]. Following gene knockout, they used the ArrayScan XTI Live High-Content Platform to show that cells lacking *TMEM175* exhibited unstable lysosomal pH, reduced autophagosome clearance, and decreased lysosomal enzyme activity, as well as impaired mitochondrial respiration.

Find the HCA system that fits your laboratory

High-content screening and analysis instruments from Thermo Fisher Scientific—including CellInsight CX5, CellInsight CX7, and ArrayScan platforms (Table 1)—have directly impacted every segment of biological research, from cellular and systems biology to drug discovery. These technology platforms build on a 20-year legacy of HCA instrument and software development and over 40 years of fluorescence imaging and probe development in our cell and protein analysis laboratories. To learn more about our high-content instrument platforms, software, applications, and analysis reagents, or to request an in-lab demonstration of one of our HCA instruments, visit **thermofisher.com/hcabp76**. ■

References

1. Love MS, Beasley FC, Jumani RS et al. (2017) *PLoS Negl Trop Dis* 11:e0005373.
2. Summermatter S, Bouzan A, Pierrel E et al. (2017) *Mol Cell Biol* 37:e00305-16.
3. Zhang J, Xiao H, Shen J et al. (2017) *Biochem Biophys Res Commun* 489:393–398.
4. Pistollato F, Canovas-Jorda D, Zagoura D et al. (2017) *Neurochem Int* 108:457–471.
5. Hill MJ, Killick R, Navarrete K et al. (2017) *J Psychiatry Neurosci* 42:181–188.
6. Lorenz C, Lesimple P, Bukowiecki R et al. (2017) *Cell Stem Cell* 20:659–674.
7. Jinn S, Drolet RE, Cramer PE et al. (2017) *Proc Natl Acad Sci U S A* 114:2389–2394.

Product	Quantity	Cat. No.
CellInsight™ CX5 High-Content Screening Platform	1 each	CX51110
CellInsight™ CX7 High-Content Analysis Platform	1 each	CX7A1110
CellInsight™ CX7 High-Content Analysis Platform and Store Standard Edition	1 each	CX7B1112
CellInsight™ CX7 High-Content Analysis Platform and Store Standard Edition plus Robotic Plate Handling	1 each	CX7C1115

Appetite for destruction

Studying macroautophagy with Premo fluorescent protein–based sensors.

Autophagy is a process of cellular self-digestion that involves the segregation and delivery of cytoplasmic cargo for degradation by hydrolytic enzymes through the lysosomal machinery. Critical to healthy cell functioning, this digestion process serves not only to recycle and repurpose intracellular material but also to dispose of misfolded proteins, damaged organelles, and other superfluous or aberrant entities.

The term autophagy covers three cellular processes that all share the lysosome as the ultimate endpoint. Microautophagy requires invagination of the lysosomal membrane to engulf cytoplasmic cargo, which is then delivered into the lysosomal lumen for degradation [1]. Chaperone-mediated autophagy utilizes transport mechanisms to transmit cytosolic proteins (containing a specific motif recognized by chaperones) across the lysosomal membrane, where they are degraded by hydrolases in the lumen [1]. Macroautophagy targets a wide range of cargo types (including dysfunctional or unnecessary proteins, organelles, and other cell components) for lysosomal digestion through formation of an autophagosome, an expanding double-membrane organelle that surrounds and engulfs the targeted cellular components and subsequently fuses with the lysosome itself [1]. It is this third process, macroautophagy, that has received the most attention and resulted in the award of the 2016 Nobel Prize in Physiology or Medicine to Yoshinori Ohsumi. Here we describe current fluorescence-based tools for studying macroautophagy, including the Invitrogen™ Premo™ Autophagy Sensors.

Studying autophagy with fluorescence-based methods

Fluorescence-based tools for identifying and monitoring cellular structures or processes include synthetic fluorescent probes, fluorescent protein chimeras (Figures 1A and 1B), and primary antibodies either labeled with a fluorescent dye or detected with a fluorescent secondary antibody (Figure 1C) [2]. All three of these methods have been harnessed to detect autophagy using a variety of fluorescence instrumentation,

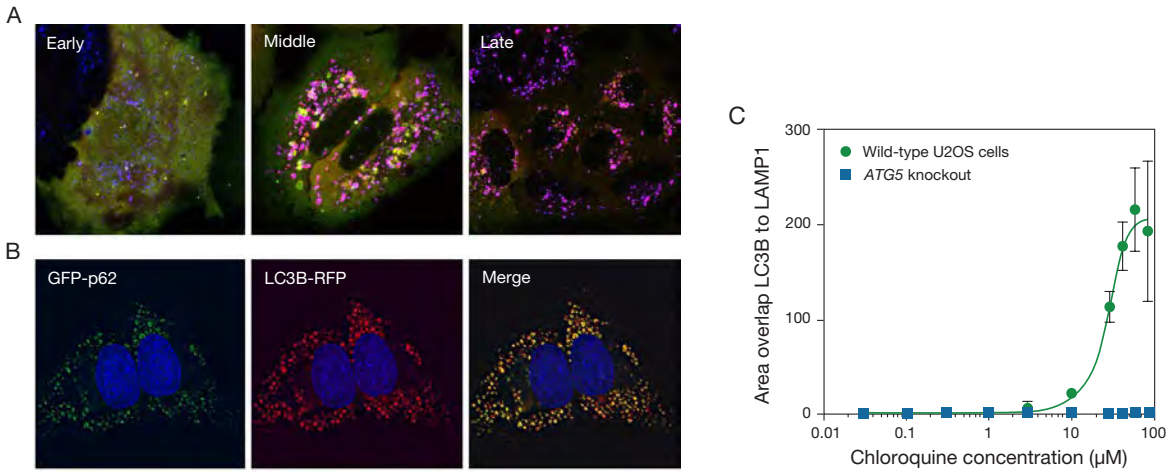

Figure 1. Detection of the autophagosomal marker LC3B using fluorescent protein chimeras or immunocytochemistry. (A) To monitor autophagosome–lysosome fusion and subsequent acidification, A549 cells were transduced with Invitrogen™ Premo™ Autophagy Tandem Sensor RFP-GFP-LC3B, stained with Invitrogen™ LysoTracker™ Deep Red dye (Cat. No. L12492), and subjected to nutrient deprivation with Gibco™ EBSS (Earle's Balanced Salt Solution, Cat. No. 14155-063). Images were captured immediately following nutrient deprivation (at 2 min, early), as well as at 20 min (middle) and 1 hr (late) after nutrient deprivation. In cells at rest (early), there are numerous discrete lysosomes (blue), with few autophagosomes (yellow puncta) or autolysosomes (pink puncta); upon nutrient deprivation, there is an increase in the number of autophagosomes (middle), followed by a decrease in the number of lysosomes and autophagosomes and an increase in the number of autolysosomes (late). **(B)** U2OS cells were transduced with Invitrogen™ Premo™ Autophagy Sensor GFP-p62 and Premo™ Autophagy Sensor LC3B-RFP and cultured for 24 hr. Chloroquine was added at a final concentration of 60 µM, and cells were cultured for a further 16 hr before counterstaining with Hoechst™ 33342 (blue). In the merged image, p62-positive protein aggregates (green) can be seen associated with LC3B-positive autophagosomes (red) and appear yellow. **(C)** Wild-type or *ATG5* knockout (KO) U2OS cells were treated with a range of chloroquine concentrations overnight to block autophagic flux. Cells were fixed, permeabilized, and then immunostained with anti-LC3B and anti-LAMP1 antibodies to label autophagosomes and lysosomes, respectively. Cells were imaged on the Thermo Scientific™ CellInsight™ CX5 High-Content Screening (HCS) Platform and analyzed with the colocalization bioapplication using Thermo Scientific™ HCS Studio™ Cell Analysis Software. Blocking autophagic flux with chloroquine leads to autolysosome accumulation in wild-type but not *ATG5* KO cells. Identification of the LC3B-positive puncta as autolysosomes is confirmed by the colocalizaiton of anti-LC3B and anti-LAMP antibodies.

and, as with all experimental approaches, they are not without caveats.

Despite the enormous breadth of proteins that can be detected using specific antibodies, immunoassays all require a similar time-consuming protocol that involves fixation, permeabilization, and blocking of the cells, followed by incubation with the primary antibody of choice and potentially a secondary antibody, with wash steps in between. The process of chemical fixation itself has been shown to affect cellular structures, leading to potential artifacts [3] and, more importantly, precludes analysis of living cells. Synthetic fluorescent dyes are popular alternatives to antibodies; however, these probes are susceptible to photobleaching and are often found not to be specific for autophagy.

An alternative to fluorescent dye– and antibody-based monitoring of autophagy is the use of cells transformed with a fluorescent protein chimera (i.e., a biosensor that contains both a fluorescent protein and a functional autophagy marker). Once generated, stable cell lines are ready to assay; however, the process of generating stably transformed cell lines is expensive and time consuming, and assaying different cell types requires the creation of new cell lines. Fortunately, the delivery of fluorescent protein–based sensors can be performed quickly and easily using the BacMam gene delivery and expression system, which is incorporated in the Invitrogen™ Premo™ Autophagy Sensor Kits. The add-and-read Premo reagents can be used to transiently transduce cells with a simple overnight incubation, after which the cells are ready to be used in autophagy assays.

Five Premo Autophagy Sensors…

The Premo Autophagy Sensors combine the specificity and live-cell compatibility of fluorescent protein–based reporters with easy delivery and expression using the BacMam gene delivery platform. Premo sensors are available as GFP (i.e., Emerald GFP) or RFP (i.e., TagRFP) constructs with either the autophagosomal marker LC3B or the autophagy receptor p62 (SQSTM1) (Figures 1 and 2). These Premo sensors can be combined with fluorescent markers of specific cargo to image its sequestration by the autophagosome (Figure 1A). Alternatively, the Premo LC3B and Premo p62 sensors can be used together to visualize the incorporation of autophagy receptors into the autophagosome (Figure 1B). Furthermore, the Premo Autophagy Tandem Sensor RFP-GFP-LC3B—which combines the pH-sensitive fluorescence of GFP with the pH-insensitive fluorescence of RFP and the autophagosomal marker LC3B—can be used to image the maturation of the autophagosome into an autolysosome and the associated increase in acidity after lysosome fusion (Figure 1A).

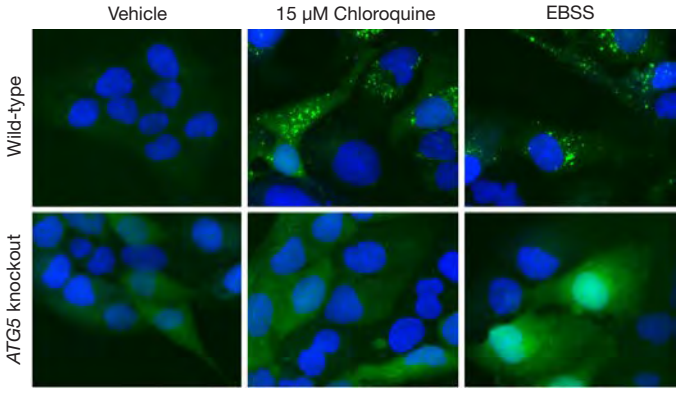

Figure 2. Specificity of labeling with Premo Autophagy Sensors. Wild-type or *ATG5* knockout (KO) U2OS cells were transduced with Invitrogen™ Premo™ Autophagy Sensor LC3B-GFP (green) and cultured for 48 hr. Cells were then incubated with vehicle or 15 µM chloroquine or subjected to nutrient deprivation with Gibco™ EBSS (Earle's Balanced Salt Solution, Cat. No. 14155-063) for 24 hr, counterstained with Hoechst™ 33342, and imaged on an Invitrogen™ EVOS™ FL Imaging System. Blocking autophagic flux with chloroquine or inducing autophagy with EBSS causes the formation of puncta (LC3B-positive autophagosomes), as compared with vehicle-treated wild-type cells. This increase in LC3B-positive puncta in response to chloroquine or EBSS is absent in *ATG5* KO cells.

… all of which are highly specific for autophagy

Of the three types of fluorescence-based autophagy tools, antibodies and fluorescent protein chimeras are the most reliable because they either bind to or mimic specific proteins involved in the autophagy pathway. When using synthetic fluorescent probes, care must be taken to ensure their specificity and determine any off-target effects using autophagy models.

Genetic models represent the most effective method for blocking the autophagy pathway (through deletion of gene products required for macroautophagy), and therefore for testing reagent specificity. In contrast, use of cell treatments that block one or more autophagy processes—e.g., inhibitors of phosphoinositide 3-kinase (PI3K), which can block the formation of autophagosomes—are typically not truly specific for autophagy because they show broad efficacy against members of multiple classes of PI3K, affecting many signaling pathways [4]. During the development of the Premo Autophagy Sensors, we used *ATG5* knockout (KO) cell lines to test for specificity. Cell lines carrying a deletion of the *ATG5* gene (encoding a protein in the Atg12–Atg5-Atg16 complex, which acts in part as an E3 ligase in the macroautophagy pathway [5]) show a loss of multiple →

macroautophagy-related events (reviewed in [6]). In cells lacking *ATG5* and transduced with Premo Autophagy Sensor LC3B-GFP, no puncta (i.e., LC3-containing autophagosomes) are seen following treatment with chloroquine to block autophagic flux or nutrient deprivation with Earle's Balanced Salt Solution (EBSS) to stimulate autophagy via mTOR inhibition (Figure 2).

Probes not specific for autophagy

Given the interest in autophagy, many fluorescent probes have been reported to be able to detect autophagosome formation, including Invitrogen™ reagents such as LysoTracker™ dyes [7], fluorescent cadaverines (e.g., monodansylcadaverine [8] and BODIPY™ TR [9] and Alexa Fluor™ derivatives [9]), and FluoZin™ ion indicators [10], as well as the CYTO-ID™ Autophagy Detection Kits (Enzo Life Sciences) [11]. Using the *ATG5* KO model, we have been able to show that these probes are not specific autophagy reporters. While many of them may report cellular events associated with autophagy, none of them can be used as specific markers for the induction of macroautophagy. For example, we observed puncta (i.e., puncta we would have concluded were autophagosomes by appearance) in *ATG5* KO cells stained with either the CYTO-ID Autophagy Detection Kit (Figure 3) or with Alexa Fluor 488 cadaverine (data not shown) following stimulation of autophagy or inhibition of autophagic flux, demonstrating the lack of specificity of these probes for macroautophagy events.

Tools for autophagy research

In addition to the Premo Autophagy Sensors, we offer a variety of lysosome-selective probes, as well as antibodies that recognize autophagy markers. Learn more about our cell analysis products for autophagy at **thermofisher.com/autophagybp76.** ■

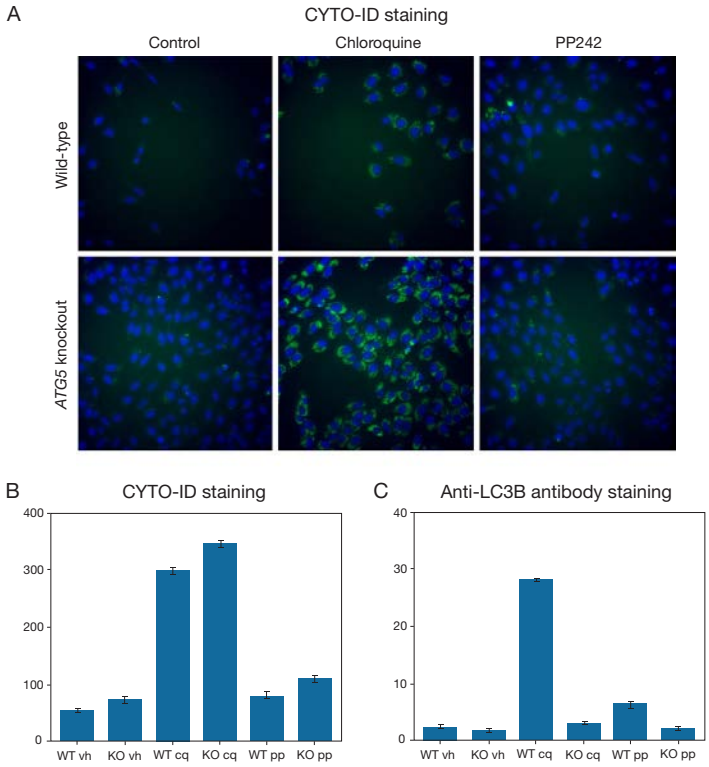

Figure 3. Use of an *ATG5* knockout cell line to determine probe specificity for macroautophagy. (A, B) Wild-type (WT) and *ATG5* knockout (KO) U2OS cells were plated, cultured for 48 hr, and stained with CYTO-ID™ Autophagy Detection Kit (Enzo Life Sciences) according to the manufacturer's instructions. As compared with treating with vehicle (vh) only, inhibiting autophagic flux with chloroquine (cq) or induction of autophagy with the mTOR inhibitor PP242 (pp) caused a significant increase in CYTO-ID staining in both wild-type and *ATG5* KO cells, indicating that the CYTO-ID probe is not specific for macroautophagy. **(C)** Following the experiments, the cells were fixed, permeabilized, and immunostained with anti-LC3B antibody (Cat. No. L10382) in the same microplate wells used for the CYTO-ID staining. LC3B immunostaining revealed that only the *ATG5* KO cells lack LC3B-positive puncta following chloroquine or PP242 treatment. Chloroquine and PP242 caused a significant increase in LC3B-positive puncta in wild-type cells.

References

1. Mizushima N, Komatsu M (2011) *Cell* 147:728–741.
2. Dolman NJ, Kilgore JA, Davidson MW (2013) *Curr Protoc Cytom* 65:12.30.1–12.30.27.
3. Schnell U, Dijk F, Sjollema KA et al. (2012) *Nat Methods* 9:152–158.
4. Mizushima N, Yoshimori T, Levine B (2010) *Cell* 140:313–326.
5. Klionsky DJ, Abdelmohsen K, Abe A et al. (2016) *Autophagy* 12:1–222.
6. Klionsky DJ, Baehrecke EH, Brumell JH et al. (2011) *Autophagy* 7:1273–1294.
7. Chikte S, Panchal N, Warnes G (2014) *Cytometry A* 85:169–178.
8. Biederbick A, Kern HF, Elsässer HP (1995) *Eur J Cell Biol* 66:3–14.
9. Huang C, Liu W, Perry CN et al. (2010) *Am J Physiol Heart Circ Physiol* 298:*H*570–*H*579.
10. Park MH, Lee SJ, Byun HR et al. (2011) *Neurobiol Dis* 42:242–251.
11. Chan LL, Shen D, Wilkinson AR et al. (2012) *Autophagy* 8:1371–1382.

Product	Quantity	Cat. No.
Premo™ Autophagy Sensor GFP-p62 Kit	1 kit	P36240
Premo™ Autophagy Sensor RFP-p62 Kit	1 kit	P36241
Premo™ Autophagy Sensor LC3B-GFP Kit	1 kit	P36235
Premo™ Autophagy Sensor LC3B-RFP Kit	1 kit	P36236
Premo™ Autophagy Tandem Sensor RFP-GFP-LC3B Kit	1 kit	P36239

Effectively monitor antibody internalization and trafficking

Improved labeling tools for antibody–drug conjugate screening and characterization.

In recent years, biotherapeutics (or biologics) have emerged as an important class of treatments that complement traditional, small-molecule drugs. Biotherapeutics comprise any therapy that utilizes a biological entity to produce it. Predominant among biotherapeutics are antibodies that can be used to modulate a specific cellular process relevant in a disease state. These antibodies confer specificity based on an extracellular epitope found only on the subset of diseased cells. Once bound to the cell surface, the antibodies can act directly to initiate apoptosis or trigger cell-mediated or complement-dependent cytotoxicity. Alternatively, the targeted antibody can be coupled to a small cytotoxic molecule to create an antibody–drug conjugate (ADC) that specifically binds an epitope on the plasma membrane and is then brought into the cell via endocytosis. Following internalization, the ADC can be trafficked to the lysosome where the drug is liberated, resulting in a highly targeted chemotherapeutic agent (Figure 1).

Given that an ADC requires endocytosis and subsequent acidification to be effective, pH-sensitive labels are very useful for following the internalization of an antibody conjugate. Fluorescein, the conventional pH-sensitive label, exhibits bright fluorescence that is quenched as the pH drops, making it a negative indicator of the acidic conditions of the endocytic pathway. In contrast, the Invitrogen™ pHrodo™ dyes display very low fluorescence at neutral pH and exhibit increasing fluorescence as the pH becomes more acidic, providing a positive indication of endocytosis

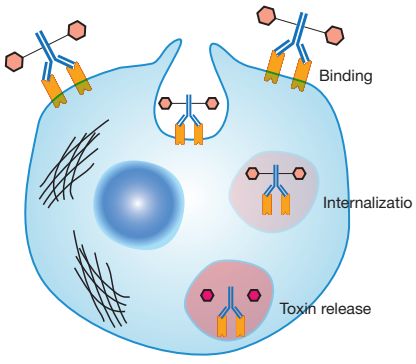

Figure 1. Internalization of an antibody–drug conjugate. An antibody–drug conjugate (ADC) comprises a monoclonal antibody directed against a tumor cell antigen coupled to a small cytotoxic molecule. An ADC is designed to specifically bind to target cells, where it is rapidly internalized. Typically the drug is liberated following trafficking to the lysosome, resulting in a highly targeted chemotherapeutic agent.

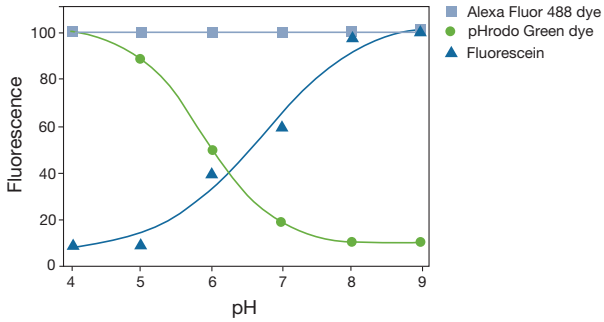

Figure 2. Comparative pH response of pH-insensitive Alexa Fluor 488 dye and pH-sensitive pHrodo Green dye and fluorescein. The Invitrogen™ Alexa Fluor™ 488 dye exhibits relatively constant fluorescence across a range of pH levels, whereas the fluorescence of fluorescein and Invitrogen™ pHrodo™ Green dye is significantly affected by pH. As the pH becomes more acidic, the fluorescence of fluorescein is quenched while the fluorescence of the pHrodo dye increases.

(Figure 2). When monitoring the internalization of a pHrodo dye–labeled antibody, the increase in pHrodo fluorescence is an effective tool, both for screening antibody candidates when creating new ADCs and for characterizing existing ADCs. An additional advantage of labeling with pHrodo dyes is that they eliminate the need for wash steps and quencher dyes to block any non-internalized dye fluorescence because they are not significantly fluorescent at the neutral pH found outside of cells.

Labeling antibodies with pH-sensitive pHrodo dyes

Traditional antibody labeling protocols can require significant optimization and often result in heterogeneous dye attachment. Moreover, when using reactive forms of fluorophores (e.g., thiol- or amine-reactive fluorescent dyes), the antigen binding site can be blocked during the labeling process, rendering the antibody ineffective. To overcome these complications, we have developed a suite of antibody labeling tools that incorporate the classic pH-insensitive, bright and photostable Invitrogen™ Alexa Fluor™ dyes, as well as the new pH-sensitive pHrodo iFL dyes. Labeling antibodies with Alexa Fluor dyes can provide a useful control in internalization experiments because the Alexa Fluor label will remain brightly fluorescent throughout the endocytosis process, from binding to internalization, regardless of the pH (Figure 2). The next-generation pHrodo iFL Green and pHrodo iFL Red dyes →

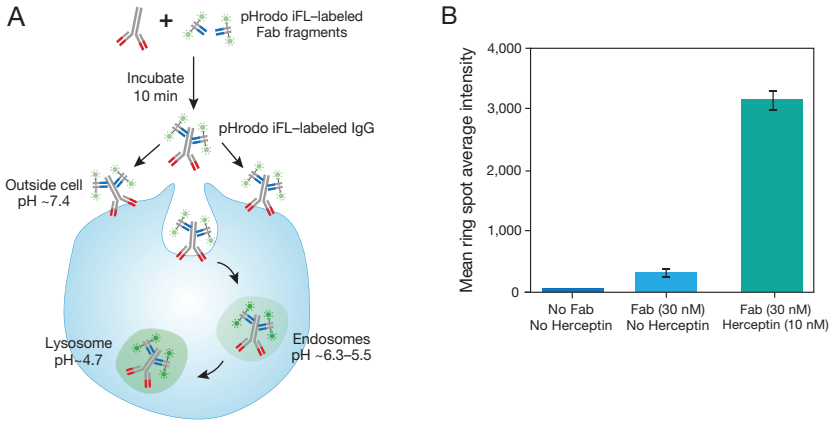

Figure 3. Zenon antibody labeling for following antibody internalization. (A) Invitrogen™ Zenon™ Antibody Labeling Kits can be used to noncovalently couple a fluorescent dye to an antibody in ~10 min. Unconjugated antibodies are incubated with fluorescently labeled Fab fragments directed against the Fc portion of a human or mouse IgG antibody, leaving the antigen binding site unmodified. **(B)** The Zenon antibody labeling method was used to label Herceptin™ (trastuzumab) with Invitrogen™ pHrodo™ iFL Red–conjugated Fab fragments (Fab). After incubation with HER2-positive SKBR3 cells (expressing human epidermal growth factor receptor 2, to which Herceptin binds), the pHrodo iFL Red–labeled Herceptin conjugate began to fluoresce, indicating internalization and acidification of the pHrodo label. No significant fluorescence was seen in vehicle-treated control cells or in cells incubated with the pHrodo iFL Red–conjugated Fab fragments alone, confirming the signal specificity.

are more soluble than the original pHrodo Green and pHrodo Red dyes, making them useful for labeling antibodies that may otherwise precipitate out of solution during conjugation.

Here we will focus on two methods for labeling antibodies with the pH-sensitive pHrodo iFL dyes: the extremely fast and noncovalent Invitrogen™ Zenon™ antibody labeling technology, and the recently updated Invitrogen™ SiteClick™ click chemistry–based antibody labeling kits. Though different in their mechanisms, both of these methods label antibodies at a specific site on the Fc portion of the heavy chain, far from the antigen binding site, thus preserving the binding properties of the antibody. We also offer amine-reactive STP esters of the pHrodo iFL dyes for traditional protein conjugation at available lysine residues.

Zenon antibody labeling with pHrodo iFL dyes

The Zenon Antibody Labeling Kits provide a means of very rapidly labeling IgG antibodies (in ~10 minutes) for use in cell binding or internalization experiments. The fast, scalable Zenon labeling method employs isotype-specific Fab fragments conjugated with either pH-sensitive pHrodo iFL dyes or classic Alexa Fluor dyes. These Fab fragments are directed against the Fc portion of a human or mouse IgG antibody, leaving the antigen binding site of the target antibody intact and free from obstruction while also providing a consistent degree of labeling. Zenon technology can label as little as 1 µg of antibody, and unlike traditional labeling methods using amine- or thiol-reactive labels, the Zenon antibody labeling is compatible with bovine serum albumin (BSA) and other stabilizing proteins.

Although the interaction between the Zenon Fab fragment and the primary antibody is noncovalent, the binding is sufficiently stable to allow detection of internalization and trafficking of the conjugates within cells. This method was used to quickly and specifically label the biotherapeutic antibody Herceptin™ (trastuzumab), which is internalized in HER2-positive cells (expressing human epidermal growth factor receptor 2, to which Herceptin binds). Because of its efficient internalization, Herceptin has been used to create the HER2-targeted ADC Kadcyla™ (ado-trastuzumab emtansine), which consists of the trastuzumab antibody linked to a cytotoxic maytansinoid.

Using the Invitrogen™ Zenon™ pHrodo™ iFL Red Human IgG Labeling Kit, we labeled Herceptin with pHrodo iFL Red–conjugated Fab fragments (Figure 3A) in order to follow its internalization in HER2-positive SKBR3 cells. pHrodo iFL Red–labeled Herceptin is nonfluorescent at neutral pH outside of cells, enabling a no-wash, no-quench assay of its internalization. No nonspecific uptake was seen in cells incubated with the pHrodo iFL dye–conjugated Fab fragments alone, confirming the specificity of the signal seen in cells treated with the pHrodo iFL dye–labeled Herceptin (Figure 3B).

Expanded options for SiteClick antibody labeling

SiteClick antibody labeling technology enables simple and site-selective attachment of compounds, including fluorescent dyes or toxins, to the carbohydrate domains present on the heavy chains of essentially all IgG antibodies, regardless of isotype and host species. We recently introduced the Invitrogen™ SiteClick™ Antibody Azido Modification Kit, which can be used to create a label-ready, site-specific azido-modified antibody, without lengthy and often inefficient genetic modification. The site-specific method employed in the SiteClick modification kit uses the enzymes β-galactosidase and β-1,4-galactosyltransferase to modify the carbohydrate domain and then attach an azide-modified sugar on the

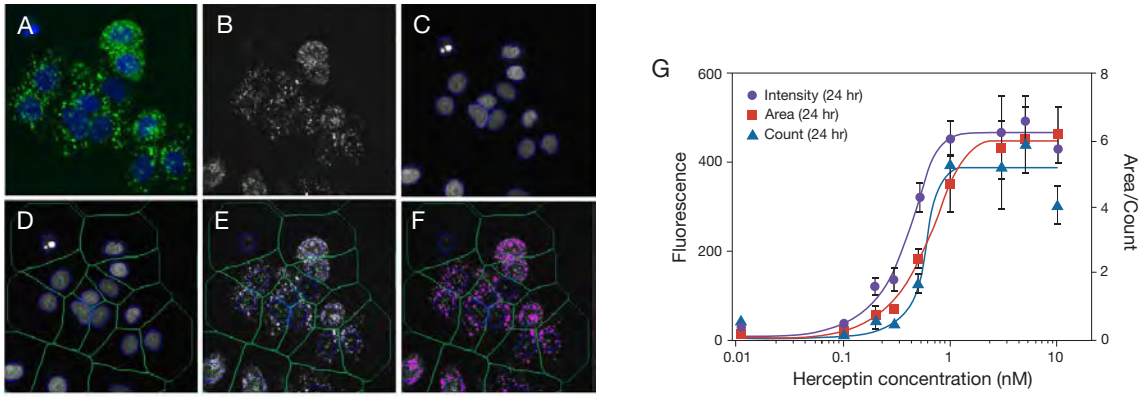

Figure 4. High-content analysis of HER2-positive cells incubated with pHrodo iFL Red–labeled Herceptin. Herceptin™ (trastuzumab) was labeled with the pH-sensitive pHrodo iFL Red dye using the Invitrogen™ SiteClick™ Antibody Azido Modification Kit in conjunction with Invitrogen™ Click-iT™ pHrodo™ Red iFL sDIBO Alkyne. HER2-positive SKBR3 cells incubated with a dose range of pHrodo iFL Red–labeled Herceptin were analyzed after 24 hr on a Thermo Scientific™ CellInsight™ CX5 High-Content Screening (HCS) Platform. **(A)** Overlay of Herceptin conjugate (green) and Hoechst™ 33342 (blue) fluorescence. **(B)** Herceptin conjugate staining alone. **(C)** Hoechst 33342 staining alone. **(D)** Cytoplasmic (ring) and nuclear (circ) segmentation with Hoechst 33342 staining. **(E)** Ring and circ overlay with Herceptin conjugate staining. **(F)** Ring, circ, and ring spot with Herceptin conjugate staining. **(G)** Over 400,000 cells were analyzed for a number of spot features using Thermo Scientific™ HCS Studio™ Cell Analysis Software—mean ring spot average intensity, mean ring spot area, mean ring spot count—in order to quantitate the fluorescence of the internalized pHrodo iFL Red–labeled Herceptin at different doses across the cell population.

heavy chains of an IgG antibody. Because the modification takes place only on the Fc portion of the heavy chains, the location and degree of labeling is very consistent and the antigen binding domains remain unaltered.

Once azido-modified, the antibody can be covalently labeled with an Invitrogen™ Click-iT™ sDIBO alkyne using copper-free click chemistry. Click-iT sDIBO alkynes are available for the pH-sensitive pHrodo iFL Red dye and the pH-insensitive Alexa Fluor dyes. Figure 4 shows HER2-positive SKBR3 cells incubated with a dose range of pHrodo iFL Red–labeled Herceptin (prepared using SiteClick labeling methods) and analyzed using the Thermo Scientific™ CellInsight™ CX5 High-Content Screening Platform, which allows quantitation of a number of parameters at a single-cell level on a large population of cells. In this experiment, over 400,000 cells were analyzed, producing a robust and reproducible data set that is particularly valuable when evaluating the performance of novel biotherapeutic antibodies across a cell population.

Find the best solution for your antibody labeling experiments

We offer a number of ready-to-use protein labeling kits for the noncovalent and covalent attachment of a broad range of intensely fluorescent dyes to your antibody or other protein, at scales from as little as 1 µg up to 3 mg IgG, including the recently introduced pHrodo iFL Microscale Protein Labeling Kits for labeling 20–100 µg of purified antibody with the amine-reactive pHrodo iFL STP ester. To learn more, visit **thermofisher.com/antbodylabelingbp76**. To see more applications of high-content imaging analysis, visit **thermofisher.com/hcabp76**. ■

Product	Quantity	Cat. No.
Zenon antibody labeling kits		
Zenon™ pHrodo™ iFL Green Human IgG Labeling Kit	1 kit	Z25611
Zenon™ pHrodo™ iFL Green Mouse IgG Labeling Kit	1 kit	Z25609
Zenon™ pHrodo™ iFL Red Human IgG Labeling Kit	1 kit	Z25612
Zenon™ pHrodo™ iFL Red Mouse IgG Labeling Kit	1 kit	Z25610
SiteClick antibody labeling kit and Click-iT sDIBO alkynes		
SiteClick™ Antibody Azido Modification Kit	1 kit	S20026
Click-iT™ Alexa Fluor™ 488 sDIBO Alkyne for Antibody Labeling	1 kit	C20027
Click-iT™ Alexa Fluor™ 555 sDIBO Alkyne for Antibody Labeling	1 kit	C20028
Click-iT™ Alexa Fluor™ 647 sDIBO Alkyne for Antibody Labeling	1 kit	C20029
Click-iT™ pHrodo™ iFL Red sDIBO Alkyne for Antibody Labeling	1 kit	C20034
Amine-reactive pHrodo iFL dyes		
pHrodo™ iFL Green Microscale Protein Labeling Kit	3 labelings	P36015
pHrodo™ iFL Green STP Ester (amine-reactive)	3 x 100 µg 1 mg	P36013 P36012
pHrodo™ iFL Red Microscale Protein Labeling Kit	3 labelings	P36014
pHrodo™ iFL Red STP Ester (amine-reactive)	3 x 100 µg 1 mg	P36011 P36010

Investigate atherosclerosis with modified low-density lipoproteins

Fluorescently labeled oxidized LDLs and acetylated LDLs.

Alterations in lipid metabolism are known to be the root defect in atherosclerosis. Atherosclerosis is a form of arteriosclerosis in which the thickening and loss of elasticity of the artery walls is caused by the buildup of fatty plaques—composed mainly of cholesterol and other lipids in blood vessels—that inhibit or block the blood flow. The exact mechanism of atherogenesis is still subject to much debate, but high levels of low-density lipoproteins (LDLs) are considered a risk factor for atherosclerosis, and high levels of high-density lipoproteins (HDLs) appear to offer some protection.

As one of the key lipid–protein complexes in blood, LDLs are responsible for the transport and delivery of lipids, including cholesterol, triglycerides, and phospholipids, throughout the body via receptor-mediated endocytosis. Modified LDLs no longer bind to the LDL receptor and are typically cleared through "scavenger" receptors on macrophages and endothelial cells. Fluorescent conjugates of LDL (native and modified) can be employed to study these pathways using fluorescence microscopy, high-content analysis, and flow cytometry. Thermo Fisher Scientific offers unmodified LDLs and their fluorescent conjugates for studying LDL receptor–mediated endocytosis and other aspects of lipid metabolism. Here we focus on two sets of fluorescently labeled, modified LDLs—oxidized LDLs and acetylated LDLs—for investigating the scavenger receptor–mediated endocytic pathways.

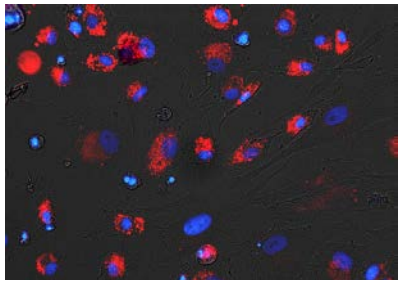

Figure 1. Endocytosis of DiI OxLDL by BPAECs. BPAECs (bovine pulmonary artery endothelial cells) were grown in poly-D-lysine–coated 96-well plates for 24 hr and then serum-starved overnight in Gibco™ FluoroBrite™ DMEM (Cat. No. A1896702) plus 0.3% BSA. On the day of the experiment, 10 µg/mL DiI OxLDL (Cat. No. L34358) was added to the medium and cells were incubated for 3 hr. After this incubation, cells were rinsed with assay buffer plus 0.3% BSA and fixed in 4% formaldehyde. Following nuclear staining with Invitrogen™ NucBlue™ Live ReadyProbes™ Reagent (Cat. No. R37605), images were acquired on the Thermo Scientific™ CellInsight™ CX5 High-Content Screening Platform.

Oxidized LDLs mimic naturally occurring processes

Oxidation of LDL is a naturally occurring process within the body, thought to be caused by the presence of free radicals. Endothelial cells and then macrophages are called into action to rid the body of oxidized LDL (OxLDL), which triggers inflammatory and immunogenic responses. Unlabeled and fluorescent OxLDL probes are therefore important tools for the study of scavenger receptor–mediated endocytosis by macrophages and endothelial cells (Figure 1), as well as the formation of macrophage-derived foam cells, a hallmark of early atherogenesis [1].

Our unlabeled OxLDL probe is generated by oxidizing the surface lipids of native or unmodified LDL using a copper sulfate incubation. During this incubation, the oxidation is continuously monitored by measuring the optical density at 234 nm [2,3]. The incubation is terminated at approximately the halfway point during the lipid peroxidation phase (Figure 2A). This oxidation level represents TBAR (thiobarbituric acid–reactive) values of approximately 25–35 nmol/mg protein. The electrophoretic mobility of this type of OxLDL preparation is found to be at least twice that of native LDL (Figure 2B). This very controlled oxidation procedure ensures that primarily lipids on the surface of the LDL are oxidized, with very limited oxidation of the surface apolipoprotein, in order to induce a physiologically relevant inflammatory response from cells.

After the proper level of oxidation is achieved and tested, fluorescently labeled OxLDL is generated by labeling with the lipid membrane intercalator DiI (1,1′-dioctadecyl-3,3,3′,3′-tetramethylindocarbocyanine perchlorate or $DiIC_{18}(3)$). DiI is a highly fluorescent lipophilic dye that can diffuse into the hydrophobic portion of the LDL complex without affecting the LDL-specific binding of the apolipoprotein. The degree of labeling in the DiI-OxLDL probe has been optimized to produce superior sensitivity in fluorescence imaging applications (Figure 1), as well as in flow cytometry and high-content imaging analyses. Each lot is analyzed for degree of labeling and functionally tested with bovine pulmonary artery endothelial cells (BPAECs) to help ensure that the oxidized probe

is recognized by scavenger receptors (Figures 1 and 3). This extensive quality testing makes it possible to achieve similar results from lot to lot, experiment to experiment.

Acetylated LDLs for specific scavenger receptors

The scavenger pathways in macrophages and endothelial cells, and the formation of foam cells, have been traditionally studied using acetylated LDL (AcLDL). Unlike the oxidation of LDL, which primarily involves modification of the surface lipids, the acetylation of LDL alters the single copy of apolipoprotein B100 on the surface of the LDL. When AcLDL complexes accumulate within macrophages and endothelial cells, the cells assume an appearance similar to that of foam cells found in atherosclerotic plaques. However, Wang and coworkers have reported that native LDL, OxLDL, and AcLDL are each trafficked to different endosomes and accumulate in distinct lysosomal compartments, indicating different endocytic pathways [4].

Thermo Fisher Scientific offers several different fluorescent AcLDL derivatives that can be used on a variety of fluorescence-based platforms. DiI AcLDL is routinely used to identify endothelial and microglial cells in primary cell cultures (Figure 4). The Invitrogen™ Alexa Fluor™ 488, Alexa Fluor™ 594, and BODIPY™ FL AcLDL derivatives may be preferred in some applications because the dyes are covalently bound to the modified apolipoprotein portion of the LDL complex and are therefore not extracted during subsequent manipulations of the cells. Given the rich publication history for both OxLDL and AcLDL, researchers can choose the appropriate modification for their particular studies and experimental setup.

Lipid droplets in foam cells

The study of foam cells plays an important role in dissecting the mechanism of atherosclerosis and developing the next generation of drugs that reduce the risk of coronary heart disease. The lipid droplets that accumulate in these foam cells are typically detected using neutral lipid stains. With an extremely high affinity for neutral lipid droplets, the Invitrogen™ HCS LipidTOX™ neutral lipid stains were developed to detect intracellular lipid droplets or globules and characterize the effects of drugs and other compounds on lipid metabolism in mammalian cell lines. These reagents are added after cell fixation (Figure 5), →

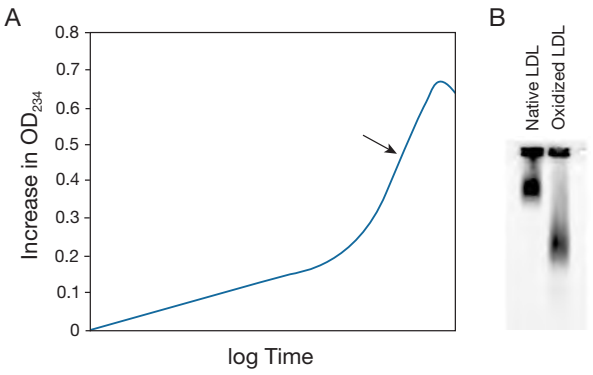

Figure 2. Real-time monitoring of the formation of OxLDL. (A) The generation of OxLDL is continuously monitored by measuring the optical density at 234 nm (OD_{234}) with a Thermo Scientific™ NanoDrop™ Spectrophotometer during the incubation of native LDL with copper sulfate. The incubation is terminated during the lipid peroxidation phase (indicated by the arrow), and the OxLDL lot is collected for further treatment. **(B)** Electrophoretic mobility of oxidized LDL (OxLDL) is at least two times greater than the mobility of native LDL.

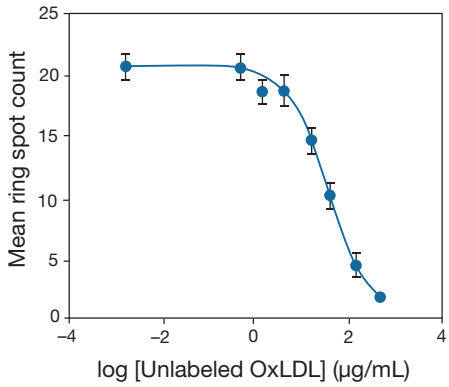

Figure 3. Specificity of DiI OxLDL for the OxLDL receptor, as determined by competitive inhibition. Bovine pulmonary artery endothelial cells (BPAECs) were plated in poly-D-lysine–coated 96-well plates for 24 hr and then serum-starved overnight in Gibco™ FluoroBrite™ DMEM (Cat. No. A1896702) plus 0.3% BSA. On the day of the experiment, cells were pretreated with a dilution series of unlabeled OxLDL (from 0 to 500 µg/mL) for 30 min at 37°C, labeled with 10 µg/mL DiI OxLDL (Cat. No. L34358) for 3 hr in a cell culture incubator, rinsed with assay buffer plus 0.3% BSA, and fixed in 4% formaldehyde. Following nuclear staining with Hoechst™ dye, images were acquired and enumerated on the Thermo Scientific™ CellInsight™ CX5 High-Content Screening Platform. Data analysis was performed with the internalization and spot count module in the Thermo Scientific™ HCS Studio™ Cell Analysis Software to quantify the number of label-positive spots per cell. Five hundred cells were sampled per well, with n = 3 wells per data point.

making them compatible with immunocytochemistry protocols, and they do not require subsequent wash steps after incubation with the sample. In addition, they are more sensitive and photostable than traditional neutral lipid stains such as Invitrogen™ BODIPY™ 493/503 dye or Nile Red, and are available with green, red, and deep red fluorescence emission.

Learn more about our LDL probes

Thermo Fisher Scientific offers the most complete portfolio of unlabeled and fluorescently labeled native LDL, OxLDL, and AcLDL for the study of lipid metabolism by fluorescence imaging, high-content analysis, and flow cytometry. All of our LDL products are derived from human LDLs isolated from human plasma, which is sourced from a blood bank and tested for HIV, hepatitis B and C, syphilis, and other infectious diseases. Visit **thermofisher.com/cellanalysisbp76** to see a summary of our cell analysis products by application, as well as our diverse collection of instrument platforms, including the Invitrogen™ EVOS™ Imaging Systems, the Thermo Scientific™ CellInsight™ High-Content Analysis Platforms, and the Invitrogen™ Attune™ NxT Flow Cytometer. ■

References

1. Xu S, Huang Y, Xie Y et al. (2010) *Cytotechnology* 62:473–481.
2. Parthasarathy S, Augé N, Santanam N (1998) *Free Radic Res* 28:583–591.
3. Ray K, Fahrmann J, Mitchell B et al. (2015) *Pain* 156:528–539.
4. Wang MD, Kiss RS, Franklin V et al. (2007) *J Lipid Res* 48:633–645.

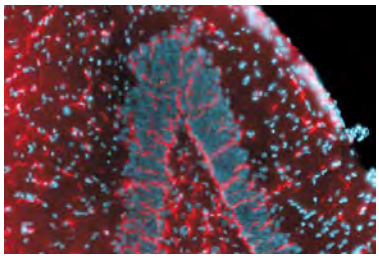

Figure 4. Microglial cells in a rat hippocampus cryosection labeled with DiI AcLDL. Microglial cells in a rat hippocampus cryosection were labeled with red-orange–fluorescent DiI AcLDL (Cat. No. L3484) and counterstained using blue-fluorescent DAPI nucleic acid stain (Cat. No. D1306).

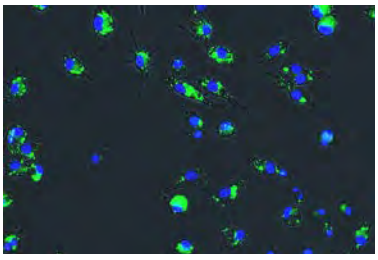

Figure 5. Accumulation of lipid droplets in RAW cells treated with OxLDL. RAW cells grown on MatTek dishes were serum-starved overnight and treated with 50 µg/mL unlabeled OxLDL (Cat. No. L34357) for 24 hr. Serum medium was then added back to the cells overnight, and cells were fixed in 4% formaldehyde and stored at 4°C. On the day of the experiment, cells were rinsed in PBS, stained with Invitrogen™ NucBlue™ Live ReadyProbes™ Reagent (Cat. No. R37605) and Invitrogen™ HCS LipidTox™ Green Neutral Lipid Stain (Cat. No. H34475) for 30 min, and rinsed in PBS again. Images were collected on an Invitrogen™ EVOS™ FL Auto 2 Imaging System at 10x magnification.

Product	Ex/Em*	Quantity	Cat. No.
Unmodified low-density lipoproteins			
Low-Density Lipoprotein from Human Plasma (LDL)	NA	200 µL	L3486
Low-Density Lipoprotein from Human Plasma, BODIPY™ FL complex (BODIPY™ FL LDL)	515/520	200 µL	L3483
Low-Density Lipoprotein from Human Plasma, DiI complex (DiI LDL)	545/571	200 µL	L3482
Low Density Lipoprotein from Human Plasma, pHrodo™ Green conjugate (pHrodo™ Green LDL)	509/533	200 µL	L34355
Low Density Lipoprotein from Human Plasma, pHrodo™ Red conjugate (pHrodo™ Red LDL)	560/585	200 µL	L34356
Oxidized low-density lipoproteins			
Low Density Lipoprotein from Human Plasma, Oxidized (OxLDL)	NA	200 µL	L34357
Low Density Lipoprotein from Human Plasma, Oxidized, DiI complex (DiI-OxLDL)	545/571	200 µL	L34358
Acetylated low-density lipoproteins			
Low-Density Lipoprotein from Human Plasma, Acetylated (AcLDL)	NA	200 µL	L35354
Low-Density Lipoprotein from Human Plasma, Acetylated, Alexa Fluor™ 488 conjugate (Alexa Fluor™ 488 AcLDL)	495/519	200 µL	L23380
Low-Density Lipoprotein from Human Plasma, Acetylated, Alexa Fluor™ 594 conjugate (Alexa Fluor™ 594 AcLDL)	590/617	200 µL	L35353
Low-Density Lipoprotein from Human Plasma, Acetylated, DiI complex (DiI AcLDL)	545/571	200 µL	L3484
Neutral lipid stains			
HCS LipidTOX™ Green Neutral Lipid Stain, for cellular imaging	495/505	1 each	H34475
HCS LipidTOX™ Red Neutral Lipid Stain, for cellular imaging	577/609	1 each	H34476
HCS LipidTOX™ Deep Red Neutral Lipid Stain, for cellular imaging	637/655	1 each	H34477

*Approximate fluorescence excitation (Ex) and emission (Em) maxima, in nm. NA = not applicable.

Double vision: Simultaneous visualization of protein and RNA targets

ViewRNA Cell Plus Assay for antibody labeling and *in situ* hybridization in individual cells.

The complex interactions between transcription, translation, and posttranslational modifications are hidden from view in typical endpoint assays that measure either RNA or protein levels. While *in situ* hybridization (ISH) provides a method for examining the levels of specific RNA transcripts in individual cells, and immunocytochemistry (ICC) utilizes antibodies to visualize the localization of specific proteins (and protein modifications), the ability to simultaneously observe RNA and protein in a single cell has been thwarted by the incompatibility of ICC and ISH protocols and the inherent lack of sensitivity of traditional ISH methods for detecting low-abundance RNA species. Further complicating these analyses, commonly used ISH protocols have limited multiplexing capability, which further constrains its compatibility with other cell assays.

The Invitrogen™ ViewRNA™ Cell Plus Assay is a novel method that combines ViewRNA ISH technology—a proprietary fluorescent *in situ* hybridization (FISH) and sequential branched DNA (bDNA) amplification technique—with antibody-based protein detection to simultaneously visualize RNA and protein in individual cells (Figure 1). The ViewRNA Cell Plus Assay enables detection of up to three RNA targets (with single-molecule sensitivity thanks to the amplification protocol) in combination with immunophenotyping for cell-surface and intracellular proteins using both indirect and direct ICC, allowing an in-depth characterization of specific cell subpopulations.

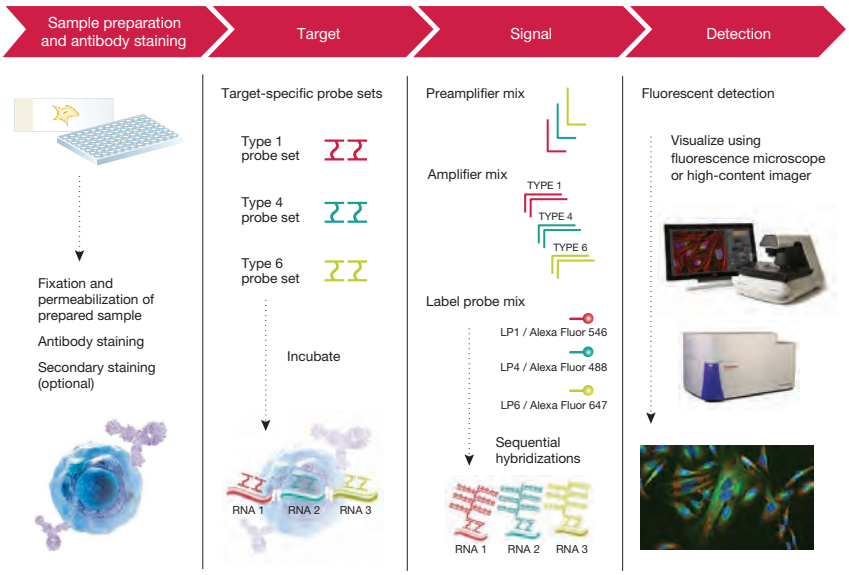

Figure 1. The ViewRNA Cell Plus Assay workflow. The workflow for the Invitrogen™ ViewRNA™ Cell Plus Assay Kit (Cat. No 88-19000-99) starts with fixation, permeabilization, and antibody labeling, followed by hybridization with RNA-specific target probes. This hybridization is then detected after branched DNA (bDNA) signal amplification using preamplifiers, amplifiers, and label probes. Labeled cells are analyzed on a fluorescence microscope or high-content imager.

A closer look at ViewRNA technology

Traditional FISH techniques that use large oligonucleotide sequences labeled with one to five fluorophores are generally limited by high background and low sensitivity due to non-specific binding and insufficient signal amplification. ViewRNA ISH assays incorporate a proprietary probe set design and bDNA signal amplification technology. A target-specific probe set of approximately 5 to 40 oligonucleotide pairs hybridizes to the target RNA of interest. An individual probe pair contains two oligonucleotides that are designed to bind adjacent to each other on the RNA transcript for bDNA signal amplification to take place. Signal amplification is achieved through a series of sequential hybridization steps with preamplifiers, amplifiers, and the fluorophore-conjugated label probes. The preamplifier molecules confer an additional level of specificity because they will hybridize to the RNA target only after both members of the oligonucleotide target probe set have bound to their target sequence. Multiple amplifier molecules subsequently hybridize to their respective preamplifier molecules. Finally, label probe oligonucleotides, which are conjugated to a fluorescent dye, hybridize to their corresponding amplifier molecules. A fully assembled signal amplification "tree" has 400 label probe binding sites. When all target-specific oligonucleotides in the probe set bind to the target RNA transcript, 8,000- to 16,000-fold amplification can be achieved.

As compared with traditional FISH, the ViewRNA ISH assays produce greater →

specificity, lower background, and higher signal-to-noise ratios. For example, to create images with similar discernible spots, traditional FISH techniques can require a 600-fold longer exposure and a 100-fold greater camera gain than ViewRNA ISH assays. Thus, under equivalent imaging conditions, the ViewRNA ISH assay is 100 times brighter than traditional FISH assays, with a two to three times higher signal-to-noise ratio [1].

The ViewRNA Cell Plus Assay workflow

The ViewRNA Cell Plus Assay workflow consists of four steps: 1) fixation, permeabilization, and antibody staining (with optional secondary antibody signal amplification), 2) RNA target probe hybridization, 3) signal amplification using bDNA constructs, and 4) detection using a standard epifluorescence microscope or high-content imaging system. Figure 1 depicts hybridization with three different target probe sets for multiplex detection of three target RNAs.

In step 1, adherent cells or centrifuged suspension cells are fixed and permeabilized prior to detection of surface or intracellular proteins. The cells are then stained with unconjugated, biotinylated, or fluorescent primary antibodies, followed by fluorescent secondary reagents if needed. In our development of the ViewRNA Cell Plus Assay, we assessed a broad panel of ICC-compatible antibodies specific for structural proteins, transcription factors, organelles, and surface markers. Our results show that signal intensity and resolution produced by the ViewRNA Cell Plus Assay is comparable to that produced by standard ICC protocols. Antibody compatibility with this assay should be verified using the Invitrogen™ ViewRNA™ Cell Plus Fixation/Permeabilization Buffer Set, and antibodies should be titrated for optimal performance, as in all ICC experiments. After an additional fixation step, the cells are ready to proceed through the RNA hybridization and signal amplification steps.

The RNA hybridization step (step 2) and subsequent bDNA amplification (step 3) require an RNA-specific target probe set containing 5 to 40 oligonucleotide pairs that hybridize to adjacent regions in the target RNA. Three types of target probe sets are currently available for RNA detection, namely Type 1, which is labeled with Invitrogen™ Alexa Fluor™ 546 dye (Ex/Em = 556/573 nm), Type 4, which is labeled with Invitrogen™ Alexa Fluor™ 488 dye (Ex/Em = 495/519 nm), and Type 6, which is labeled with Invitrogen™ Alexa Fluor™ 647 dye (Ex/Em = 650/668 nm). When detecting more than one RNA target in a single sample, each target probe set must be a unique type to differentiate its signal from the others. Once the cells have been processed by the ViewRNA Cell Plus Assay, the data can be collected and analyzed on an epifluorescence microscope or high-content imaging system equipped with the appropriate filter sets (step 4).

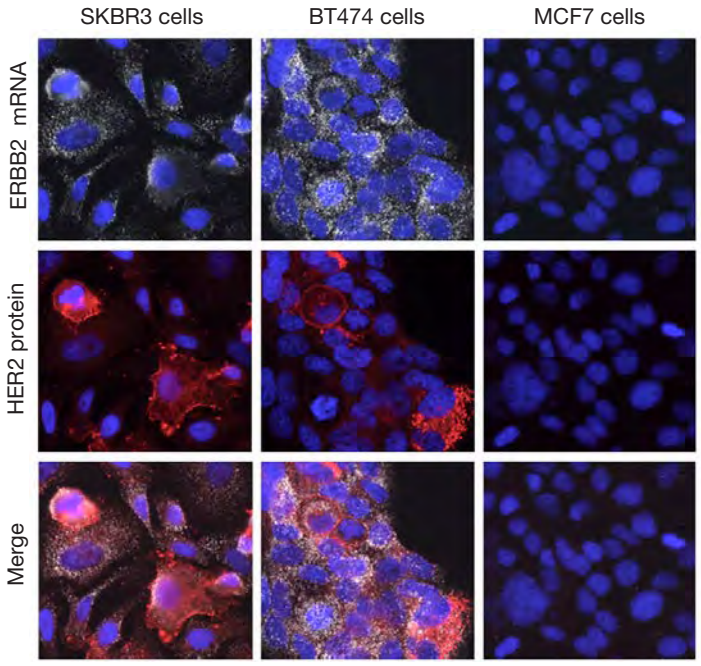

Figure 2. Use of the ViewRNA Cell Plus Assay to examine ERBB2 mRNA and HER2 protein expression levels simultaneously in three different human breast cancer cell lines. Using the Invitrogen™ ViewRNA™ Cell Plus Assay Kit (Cat. No. 88-19000-99), we labeled the HER2 protein with an Invitrogen™ eBioscience™ eFluor™ 570 anti–human ErbB2/HER2 antibody (Cat. No. 41-9757-82), and ERBB2 mRNA expression was assessed with a Type 6 (Alexa Fluor 647) label probe specific for ERBB2 mRNA. We observed ERBB2 mRNA (white) localized to the cytoplasm while HER2 protein (red) is found predominantly in the membrane in both SKBR3 and BT474 cells. MCF7 cells, which do not show ERBB2 gene amplification, were negative for ERBB2 mRNA and HER2 protein expression. Nuclei were stained with DAPI nucleic acid stain (blue).

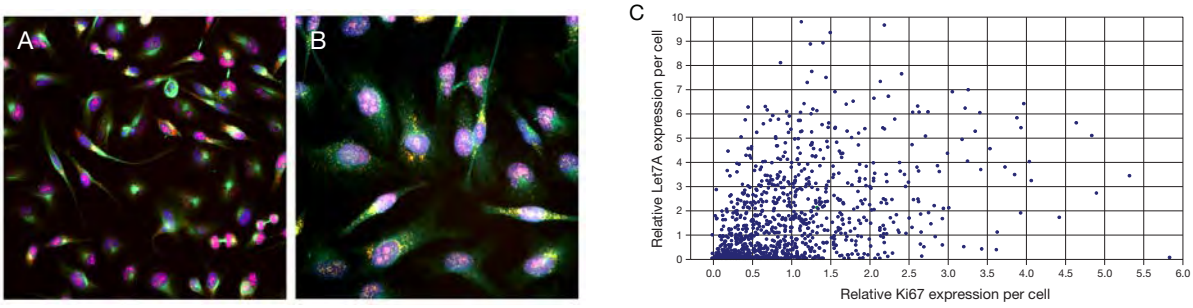

Figure 3. Use of the ViewRNA Cell Plus Assay to examine Let7A mRNA and Ki67 protein expression levels simultaneously in NIH/3T3 cells. After labeling NIH/3T3 cells with Invitrogen™ eBioscience™ eFluor™ 660 anti-Ki67 antibody to visualize Ki67 protein expression (purple), cells were hybridized with a Type 6 (Alexa Fluor 647) label probe specific for Let7A mRNA expression (yellow to red) using the Invitrogen™ ViewRNA™ Cell Plus Assay Kit (Cat. No. 88-19000-99). The cells were counterstained for tubulin (green, labeled with an anti–α-tubulin primary antibody and an Invitrogen™ Alexa Fluor™ 488 secondary antibody) and nuclei (blue, detected with DAPI nucleic acid stain). The cells were imaged using either **(A)** the Invitrogen™ EVOS™ FL Auto 2 Imaging System with a 20x objective or **(B)** the Thermo Scientific™ CellInsight™ CX7 High-Content Analysis Platform with a 40x objective. Ki67 expression (purple) is limited to the nucleus, whereas Let7A expression (yellow to red) is primarily seen in the cytoplasm. **(C)** Using Thermo Scientific™ HCS Studio™ Cell Analysis Software available with the CellInsight CX7 instrument, the relative expression of Let7A/cell was plotted vs. the relative expression of Ki67/cell (cell number = 994). This scatter plot indicates a possible relationship between expression of Let7A microRNA and the protein Ki67.

ViewRNA Cell Plus Assay in action

Although studies have shown that the correlation between levels of RNA and protein products varies widely, a general relationship between transcription level and protein presence can be used to assess the accuracy and specificity of the ViewRNA Plus Cell Assay. To show the relationship between transcription and translation, ERBB2 RNA and HER2 protein expression were visualized in several breast cancer cell lines of known HER2 status (Figure 2). SKBR3 and BT474 cells are characterized as $HER2^+$, while MCF7 cells are $HER2^-$. The data in Figure 2 demonstrate that ERBB2 mRNA is present in all cells within the SKBR3 and BT474 cultures; however, expression of HER2 protein is heterogeneous within the cell population and localizes primarily to the cell membrane, with some protein detected in the cytoplasm.

Figure 3 shows the use of the ViewRNA Cell Plus Assay for the detection of both Let7A microRNA, which is known to play a role in cell proliferation, and the protein Ki67, a proliferation marker. The expression levels of specific microRNAs, which are noncoding RNA, are particularly difficult to measure, and the bDNA amplification method used in the ViewRNA Cell Plus Assay is one of the few methods sensitive enough to detect microRNA. Cells labeled with the ViewRNA Cell Plus Assay Kit can be imaged using an epifluorescence microscope such as the Invitrogen™ EVOS™ FL Auto 2 Imaging System, or with a high-content analysis instrument such as the Thermo Scientific™ CellInsight™ CX7 High-Content Analysis Platform, which facilitates the analysis of the relative expression and colocalization of microRNA and protein at the single-cell level.

Learn more about the ViewRNA Cell Plus Assay Kit

The ViewRNA Cell Plus Assay combines highly sensitive ISH for visualizing RNA at single-molecule sensitivity with ICC for protein detection in individual cells. This assay enables simultaneous detection of up to three RNA targets in combination with immunophenotyping for cell-surface and intracellular proteins using both indirect and direct ICC. The combined visualization of RNA and protein expression at the single-cell level is a valuable tool for correlating RNA and protein levels in single cells, analyzing sample heterogeneity, tracking viral RNA and protein, and a variety of other areas of cell biology research.

The ViewRNA Cell Plus Assay Kit contains the key reagents needed to conduct the assay; target-specific probe sets for genes of interest and antibodies for protein detection are sold separately. For more information, including recent publications and customer webinars as well as available probe sets and ordering guidelines, visit **thermofisher.com/viewrnacellplusbp76**. ■

Reference

1. Battich N, Stoeger T, Pelkmans L (2013) *Nat Methods* 10:1127–1133.

Product	Quantity	Cat. No.
ViewRNA™ Cell Plus Assay Kit	1 kit	88-19000-99
ViewRNA™ Cell Plus Cytospin Module Kit	1 kit	88-19002-11
ViewRNA™ Cell Plus Fixation/Permeabilization Buffer Set	1 kit	00-19001

Maximize survival of neurons derived from primary and stem cells

Introducing the Gibco B-27 Plus Neuronal Culture System.

Functional *in vitro* studies of neurons and neural networks require that the cells be maintained for prolonged periods of time at an optimal density. For primary rodent neurons, full functionality and maturation require maintenance *in vitro* for approximately 21 days, whereas human induced pluripotent stem cell (iPSC)–derived neurons require several weeks to months in culture. For more than 25 years, scientists have relied on Gibco™ B-27™ Supplement and Gibco™ Neurobasal™ Medium for a variety of neuronal culture applications [1].

Maintain neuronal cultures longer

Scientists are now seeking to maintain a higher density of neurons over longer periods of time than B-27 Supplement and Neurobasal Medium were originally designed to support. Part of the reason for these more stringent growth conditions is the advent of human iPSC-derived neurons, which grow and mature more slowly than primary rodent neurons. To address this need, we have developed the Gibco™ B-27™ Plus Neuronal Culture System—a serum-free neuronal culture system consisting of B-27 Plus Supplement and Neurobasal Plus Medium—that reliably enables the highest survival rates of primary and stem cell–derived neurons.

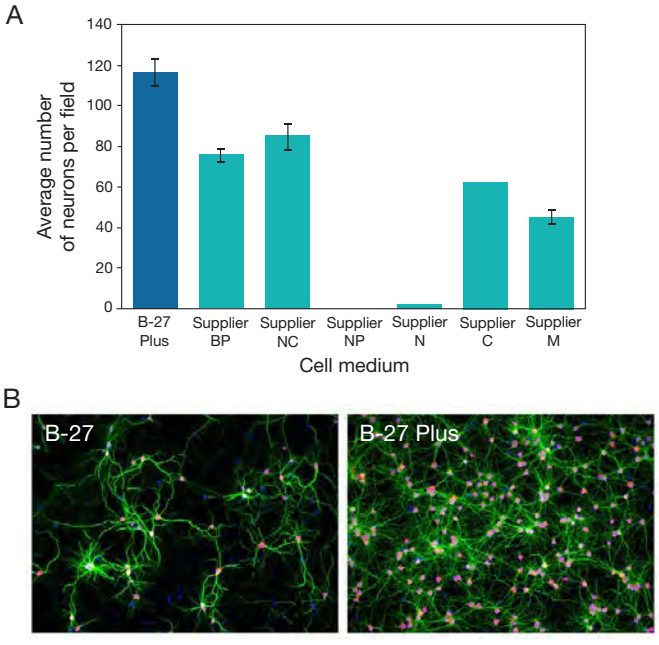

Figure 1. The B-27 Plus Neuronal Culture System promotes the highest survival rates of primary rodent neurons in culture. (A) Cryopreserved mouse cortical neurons (Cat. No. A15586) were maintained for 21 days in the indicated media. Neuronal survival was measured by immunofluorescence labeling of the neuronal somatic marker HuC/D using an anti-HuC/HuD monoclonal antibody (clone 16A11, Cat. No. A21271) in conjunction with Invitrogen™ Alexa Fluor™ 594 anti–mouse IgG secondary antibody (Cat. No. A11005). The bar graph shows the average results of three experiments in which the Gibco™ B-27™ Plus Neuronal Culture System (Cat. No. A3653401) was compared with other commercially available products. **(B)** Mouse cortical neurons, cultured for 21 days with either the B-27 Plus Neuronal Culture System or the classic B-27 Supplement and Neurobasal Medium, were immunostained for MAP2 (green) and HuC/HuD (red); nuclei were counterstained with DAPI nucleic acid stain (blue). These fluorescence images are representative fields that illustrate the improved neuronal survival using the B-27 Plus Neuronal Culture System.

Optimized formulations for neuronal culture

Leveraging our experience as the sole provider of B-27 supplements, we have optimized the formulation of B-27 Plus Supplement and Neurobasal Plus Medium, implemented more stringent requirements for raw materials, and improved our manufacturing, validation, and quality control processes. The optimized products work synergistically as a system, significantly improving upon the classic combination of B-27 Supplement and Neurobasal Medium and also outperforming other commercially available media in terms of neuronal survival and long-term maintenance (Figure 1).

In addition, the B-27 Plus Neuronal Culture System significantly accelerates neurite outgrowth in short-term neuronal cultures (Figures 2A and 2B) and improves the electrical activity in long-term cultures relative to the classic B-27 Supplement and Neurobasal Medium (Figure 2C). The accelerated neurite outgrowth and increase in spontaneous firing, together with a concomitant increase in synapsin staining (Figure 2D) for neurons grown using the B-27 Plus system, indicate the formation of functional synapses.

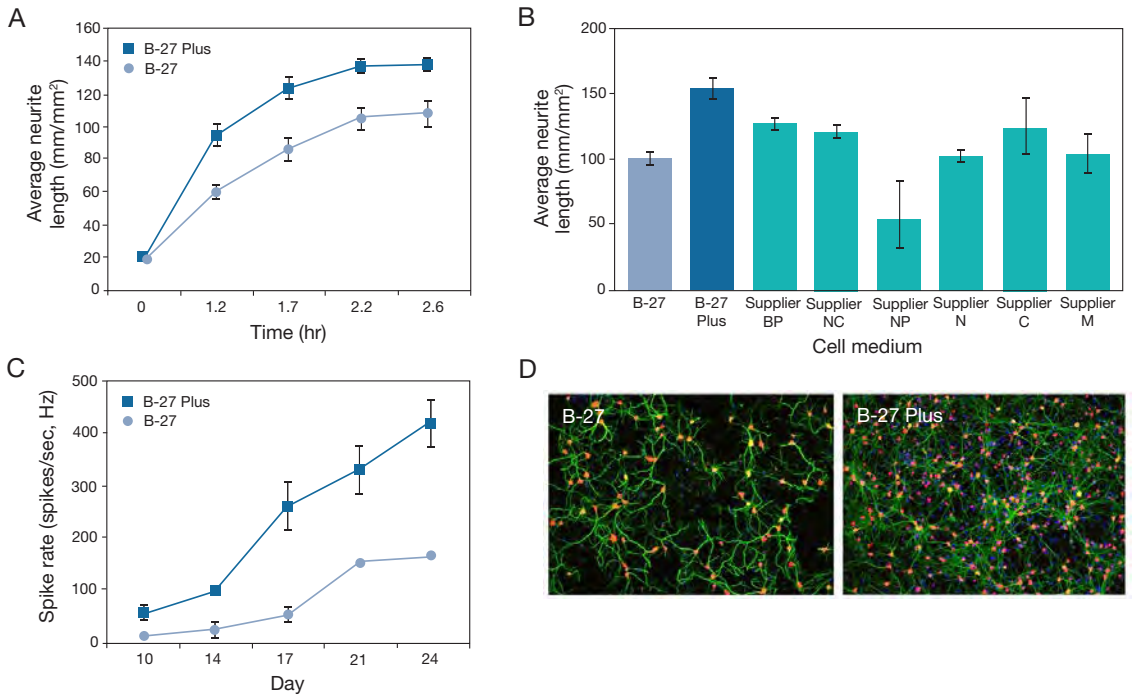

Figure 2. As compared with B-27 Supplement and Neurobasal Medium, the B-27 Plus Neuronal Culture System produces significantly improved maturation and electrical activity in primary rodent neurons. (A, B) Cryopreserved mouse cortical neurons (Cat. No. A15586) were maintained in the indicated media systems, and neurite outgrowth was quantified using differential interference contrast images. **(A)** The Gibco™ B-27™ Plus Neuronal Culture System showed accelerated neurite outgrowth when compared with that obtained using the original combination of B-27 Supplement and Neurobasal Medium. **(B)** When compared with other commercially available media systems, the B-27 Plus Neuronal Culture System also produced the longest neurite lengths after 7 days. **(C, D)** Cryopreserved rat cortical neurons (Cat. No. A1084002) were maintained for over 3 weeks in either the classic B-27 Supplement and Neurobasal Medium or the B-27 Plus Neuronal Culture System. **(C)** Cells were grown in 12-well MEA plates, and electrical activity recordings were initiated on *in vitro* day 10 and continued to day 24. The graph of spike rate vs. time shows the increase in spontaneous electrical activity from day 10 to day 24; each data point is an average of three wells. **(D)** Rat cortical neurons, cultured for 28 days with either the B-27 Plus Neuronal Culture System or the classic B-27 Supplement and Neurobasal Medium, were immunostained for MAP2 (green) and synapsin (red); nuclei were counterstained with DAPI nucleic acid stain (blue). These fluorescence images are representative fields that illustrate the increased synapse formation using the B-27 Plus Neuronal Culture System.

Learn more about B-27 Plus neuronal culture

The B-27 Plus Neuronal Culture System promotes high survival rates of primary and stem cell–derived neurons in both short- and long-term culture, which enables successful downstream applications utilizing these cells (see front cover image). In protocols used to differentiate, maintain, and mature neurons, the optimized B-27 Plus Supplement and Neurobasal Plus Medium should be used in place of the original versions of these products. The B-27 Plus Neuronal Culture System should not be used for neural stem cell expansion or in place of other specialized versions of B-27 supplements and Neurobasal media (e.g., B-27 supplements minus vitamin A or minus insulin, or Neurobasal-A media). B-27 Plus Supplement and Neurobasal Plus Medium are offered in the same volumes and concentrations as the classic products, which will continue to be available. Learn more at **thermofisher.com/b27bp76**. ■

Reference

1. Brewer GJ, Torricelli JR, Evege EK et al. (1993) *J Neurosci Res* 35:567–576.

Product	Quantity	Cat. No.
B-27 Plus neuronal culture media		
B-27™ Plus Neuronal Culture System	1 kit	A3653401
B-27™ Plus Supplement (50X)	10 mL	A3582801
Neurobasal™ Plus Medium	500 mL	A3582901
Classic B-27 neuronal culture media		
Gibco™ Neural Cell Culture Starter Kit	1 kit	A32116
B-27™ Supplement (50X), minus antioxidants	10 mL	10889038
B-27™ Supplement (50X), minus insulin	10 mL	A1895601
B-27™ Supplement (50X), minus vitamin A	10 mL	12587010
B-27™ Supplement (50X), serum free	10 mL	17504044
CTS™ B-27™ Supplement, XenoFree	10 mL	A1486701
CultureOne™ Supplement (100X)	5 mL	A3320201

T lymphocyte immunophenotyping

14-color flow cytometry panel featuring Super Bright antibody conjugates.

Here we present a 14-color immunophenotyping panel used to characterize human T lymphocytes. This analysis takes advantage of the diverse collection of fluorescent antibodies available, including those labeled with Invitrogen™ eBioscience™ Super Bright polymer dyes, a suite of exceptionally bright fluorophores excited by the violet laser. Optimized for use in flow cytometry, the Super Bright dyes allow for expanded use of violet laser excitation, promote streamlined multicolor panel design, and enable detection of low-abundance cell targets.

Recently expanded to include 6 fluorescence detectors for the violet laser (405 nm), the Invitrogen™ Attune™ NxT Flow Cytometer is capable of detecting multiple Super Bright dyes in a single immunophenotyping panel, greatly expanding the number of fluorescent parameters that can be simultaneously measured. The unique acoustic-assisted hydrodynamic focusing technology of the Attune NxT cytometer enables rapid, accurate, and sensitive detection at high flow rates without compromising data quality, as demonstrated with this 14-color data set (Figure 1).

Summary of methods and panel development

Human peripheral blood mononuclear cells (PBMCs) were prepared from whole blood using density gradient separation, and then stimulated by treating with 5 µg/mL concanavalin A for 3 days. Unstimulated cells were also tested, and fluorescence-minus-one (FMO) controls were prepared for marker boundary placement [1]. Cell samples were labeled with the optimal titer for each antibody conjugate, and single-color compensation controls were prepared using the Invitrogen™ AbC™ Total Antibody Compensation Kit for antibody conjugate compensation and Invitrogen™ ArC™ Amine-Reactive Compensation Bead Kit for compensation of the Invitrogen™ LIVE/DEAD™ Fixable Dead Cell Stain.

Table 1 shows the specifications for the 14-color T cell immunophenotyping panel, including the Attune NxT V6 instrument configuration and the panel reagents. The T cell phenotypic markers used in this panel identify differentiation profiles, activation, exhaustion status, and co-stimulatory activity. Instead of using conventional intracellular markers

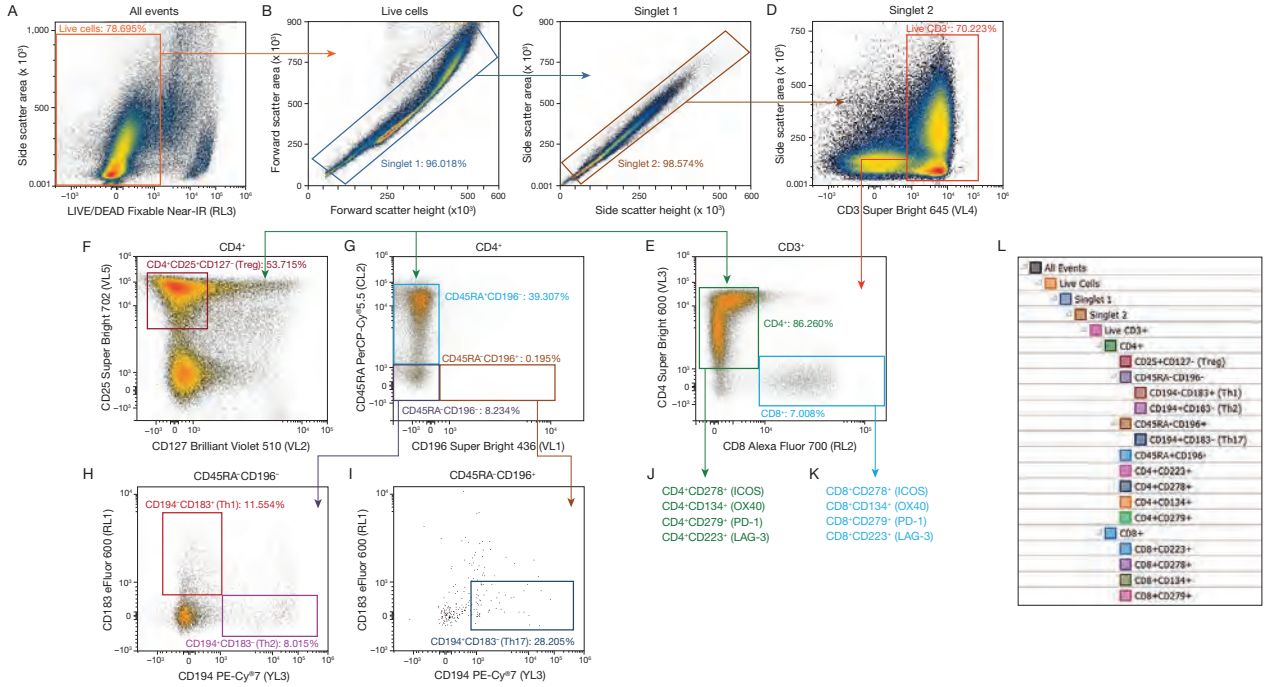

Figure 1. Gating strategy for the 14-color T lymphocyte immunophenotyping panel using the Attune NxT V6 Flow Cytometer. A region is placed around live peripheral blood mononuclear cells (PBMCs), as identified by the Invitrogen™ LIVE/DEAD™ Fixable Near-IR Dead Cell Stain **(A)**. Live cells are analyzed through sequential singlet gating **(B, C)**, and the resulting CD3⁺ population **(D)** is further delineated by gating on CD4⁺ and CD8⁺ populations **(E)**. The CD4⁺ population is used to gate on CD25 vs. CD127 **(F)**, CD45RA vs. CD196 **(G)**, and CD278, CD134, CD279, and CD223 populations (data not shown) **(J)**. The CD45RA⁻CD196⁻ population from **(G)** is gated on CD183 vs. CD194 **(H)**. The CD45RA⁻CD196⁺ population from **(G)** is gated on CD183 vs. CD194 **(I)**. The CD8⁺ population from **(E)** is used for gating CD278, CD134, CD279, and CD223 populations (data not shown) **(K)**. The entire gating strategy is displayed in hierarchical format using the Invitrogen™ Attune™ NxT V6 v2.6 software for easy visualization **(L)**.

for cytokines (e.g., IFN-γ) or transcription master regulators (e.g., T-bet), only surface markers were selected for this panel so that fixation and permeabilization steps were not required. This streamlined and shortened the sample preparation process, while also reducing cell loss due to multiple wash steps. For example, to detect T helper 1 (Th1), Th2, and Th17 subpopulations, we used the surface markers CD45RA, CD196 (CCR6), CD183 (CXCR3), and CD194 (CCR4) [2]. Likewise, T regulatory (Treg) cells, often detected with the surface marker CD25 and the intracellular marker FoxP3, were instead identified using only surface markers CD25 and CD127 [3,4]. Upon activation or in diseases such as hematologic malignancies, T cells up-regulate expression of activation markers such as CD25, CD134 (OX40), and CD278 (ICOS, inducible co-stimulator). Expression of CD279 (PD-1), an immune checkpoint receptor, is used to identify T cells as exhausted or quiescent. Another immune checkpoint receptor, CD223 (LAG-3), negatively regulates cellular proliferation, activation, and homeostasis of T cells, and plays a role in Treg suppressive activity [5]. Table 2 lists the T cell subpopulations and corresponding immunophenotypes identified by this panel.

Table 1. Specifications for the 14-color T cell immunophenotyping panel, including the Attune NxT V6 instrument configuration and the panel reagents (antibody target, clone, and fluorophore).

Laser	Attune NxT V6 detector	Bandpass filter (nm)	Target	Clone	Fluorophore	Cat. No.
Blue 488 nm	BL1	530/30	CD134 (OX40)	ACT-35	FITC	11-1347-42
	BL2	695/40	CD45RA	HI100	PerCP-Cy®5.5	45-0458-42
Red 637 nm	RL1	670/14	CD183 (CXCR3)	CEW33D	eFluor 660	50-1839-42
	RL2	720/30	CD8	RPA-T8	Alexa Fluor 700	56-0088-42
	RL3	780/60	Viability	NA	LIVE/DEAD Fixable Near-IR	L34976
Violet 405 nm	VL1	450/40	CD196 (CCR6)	R6H1	Super Bright 436	62-1969-41
	VL2	525/50	CD127	A019D5	Brilliant Violet 510	NA
	VL3	610/20	CD4	SK3	Super Bright 600	63-0047-42
	VL4	660/20	CD3	OKT3	Super Bright 645	64-0037-42
	VL5	710/50	CD25	BC96	Super Bright 702	67-0259-42
	VL6	780/60	CD279 (PD-1)	EH12.1	Brilliant Violet 786	NA
Yellow 561 nm	YL1	585/22	CD278 (ICOS)	ISA-3	PE	12-9948-42
	YL2	620/15	CD223 (LAG-3)	3DS223H	PE-eFluor 610	61-2239-42
	YL3	780/60	CD194 (CCR4)	1G1	PE-Cy®7	NA

Table 2. Summary of results from the 14-color T cell immunophenotyping panel.

		Percent (%) positive cells after 3-day stimulation with control or concanavalin A	
Immunophenotype	T cell subpopulation*	Unstimulated PBMCs	Stimulated PBMCs
$CD3^+CD4^+CD45RA^-CD196^-CD183^+CD194^-$	Th1 cells	16.74	10.88
$CD3^+CD4^+CD45RA^-CD196^-CD183^-CD194^+$	Th2 cells	3.79	6.43
$CD3^+CD4^+CD45RA^-CD196^+CD183^-CD194^+$	Th17 cells	18.79	28.21
$CD3^+CD4^+CD25^+CD127^-$	Treg cells	0.92	51.63
$CD3^+CD4^+CD223^+$	LAG-3+ exhausted Th cells	0.79	39.84
$CD3^+CD8^+CD223^+$	LAG-3+ exhausted Tc cells	0.17	37.30
$CD3^+CD4^+CD134^+$	OX40+ activated Th cells	1.08	21.26
$CD3^+CD8^+CD134^+$	OX40+ activated Tc cells	0.23	11.16
$CD3^+CD4^+CD278^+$	ICOS+ activated Th cells	0.27	18.65
$CD3^+CD8^+CD278^+$	ICOS+ activated Tc cells	0.76	14.59
$CD3^+CD4^+CD279^+$	PD-1+ exhausted/quiescent Th cells	1.36	16.12
$CD3^+CD8^+CD279^+$	PD-1+ exhausted/quiescent Tc cells	1.24	13.17

*Th = T helper cells. Treg = T regulatory cells. Tc = T cytotoxic cells.

Data acquisition and analysis

Samples were acquired on the recently introduced 4-laser Attune NxT V6 Flow Cytometer, which has the ability to detect 6 violet laser–excited fluorophores, with a flow rate of 200 µL/minute. Data were analyzed using Attune NxT v2.6 software. Corrections for spectral overlap were performed using standard instrument auto-compensation procedures. The results show well-characterized cell populations, with the expected differences between unstimulated and stimulated PBMCs *ex vivo* (Table 2).

Find more for flow cytometry

See our comprehensive suite of products for flow cytometry, from instruments and standards to antibodies and cell function reagents at thermofisher.com/flowcytometrybp76. ■

References

1. Maecker HT, Trotter J (2006) *Cytometry A* 69:1037–1042.
2. Gosselin A, Monteiro P, Chomont N et al. (2010) *J Immunol* 184:1604–1616.
3. Sakaguchi S, Miyara M, Costantino CM et al. (2010) *Nat Rev Immunol* 10:490-500.
4. Yu N, Li X, Song W et al. (2012) *Inflammation* 35:1773–1780.
5. Huang CT, Workman CJ, Flies D et al. (2004) *Immunity* 21:503–513.

Boost your stem cell antibody arsenal

Monoclonal antibodies for studying human pluripotent stem cells.

Stem cells are undifferentiated cells that have the capacity both to self-renew through mitosis and to differentiate into specialized cell types such as neurons or muscle cells. Human embryonic stem cells (hESCs) and induced pluripotent stem cells (hiPSCs) are pluripotent stem cells (hPSCs) that can divide for a long period of time in culture and have the potential to differentiate into any cell type found in the human body [1]. Both differentiated and undifferentiated stem cells are identified and characterized using primary antibodies to key targets, which are detected by fluorescence-based methods such as immunofluorescence imaging and flow cytometry. hPSCs are commonly identified using monoclonal antibodies (mAbs) that recognize cell-surface proteins, including SSEA3, SSEA4, TRA-1-60, TRA-1-81, and GCTM-1, as well as the intracellular transcription factor OCT4. The study and application of stem cells will be enhanced by the availability of well-characterized hPSC-specific mAbs detecting cell-surface epitopes.

Cell-surface markers for pluripotent stem cells

A research team from CSIRO in Australia has recently described the generation of a set of mAbs that recognize cell-surface proteins present on hESCs and hiPSCs [2]. These cell-surface proteins were previously identified in a study examining spontaneously differentiating hPSCs that were also rapidly losing immunoreactivity to two cell-surface markers (GCTM-2 and CD9) associated with human pluripotency [3]. Bioinformatic analysis of the gene signature of these cells identified 88 cell-surface proteins, most of which had not been previously associated with undifferentiated hPSCs [3]. Here we report on the characterization of four mAbs (CSTEM26, CSTEM27, CSTEM28, and CSTEM29 clones) capable of detecting these cell-surface markers on live hPSCs. An interview with Andrew Laslett, PhD, who was part of the team that developed and characterized these antibodies, is available at **thermofisher.com/stemcellabs**.

Characterizing the stem cell antibodies

Antibodies against CUB domain–containing protein 1 (CDCP1 or CD318, clone CSTEM26), platelet F11 receptor (F11R or CD321, clone CSTEM27), desmoglein 2 (DSG2, clone CSTEM28), and P-cadherin (cadherin 3 or CDH3, clone CSTEM29) were shown to be highly specific for their respective target cell-surface proteins by ELISA (data not shown), indirect immunofluorescence of fixed hESCs (Figure 1), and flow cytometry using live hPSCs (Figure 2) [2]. The specificity of the antibodies for their target cells was further verified using flow cytometry to detect their coexpression with the transcription factor OCT4 in fixed cells (Figure 3) and the cell-surface proteins TRA-1-60 and SSEA-4 in live cells (data not shown).

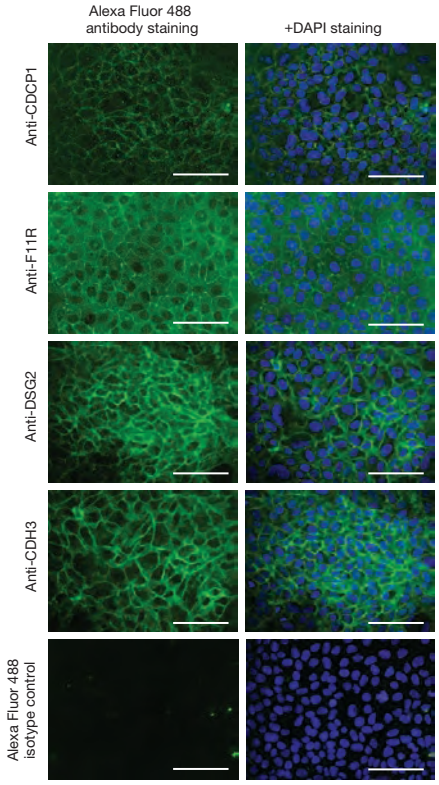

Figure 1. Immunostaining of undifferentiated MEL1 human embryonic stem cells. Undifferentiated MEL1 human embryonic stem cells (hESCs) cultured on a feeder layer of mouse embryonic fibroblasts in human pluripotent stem cell (hPSC) medium for 4–7 days were fixed in cold 100% ethanol and surface-labeled with anti-CDCP1 (Cat. No. 14-3189-80), anti-F11R (Cat. No. 14-3219-80), anti-DSG2 (Cat. No. 14-9159-80), or anti-CDH3 (Cat. No. 14-2237-80) monoclonal antibodies (or the corresponding isotype control) in conjunction with Invitrogen™ Alexa Fluor™ 488 secondary antibodies (green), counterstained with DAPI nucleic acid stain (blue), and imaged by fluorescence microscopy. Scale bars = 100 µm.

Additional studies have demonstrated that these new antibodies can be used to sort and enrich hPSCs for use with transcriptome or differentiation studies. Cells with high expression of the target proteins were sorted by fluorescence-activated cell sorting (FACS) and re-plated to form self-renewing cell colonies that contain high percentages of OCT4-positive hPSCs (data not shown) [2].

Fluorescent conjugates of the antibodies against CDCP1, F11R, and CDH3 were shown to detect a high percentage of the TRA-1-60–positive cells from a mixture of hiPSCs and the murine C2C12 cell line, demonstrating their use for identifying hiPSCs in mixed-cell populations. These antibodies also appear to have uses not directly associated with pluripotency. For example, anti-CDCP1, anti-F11R, and anti-DSG2 were shown to detect antigen expression on human breast epithelial and stromal subpopulations by flow cytometry (data not shown) [2], suggesting potential as breast cancer biomarkers.

Selection tools for stem cell antibodies

Characterization of stem cells is a critical step in stem cell research. The mAbs reported here—exclusively available through the Invitrogen™ antibody portfolio—add to our set of stem cell antibodies for detecting and purifying subpopulations of stem cells, for enriching hPSCs before differentiation, and for conducting quantitative comparisons of hPSC lines. No matter which detection platform you use—flow cytometry, microscopy, western blotting, ELISA, or other—the collection of over 40,000 antibodies from Thermo Fisher Scientific provides you with choices compatible with your experimental design. Visit **thermofisher.com/antibodiesbp76**, where you will find an antibody search tool that allows you to filter by target, antibody type, application, and host species. ■

Antibody target	Clone	Format	Quantity	Cat. No.
CD318 (CDCP1)	CSTEM26	Unconjugated	25 µg	14-3189-80
			100 µg	14-3189-82
		PE	25 tests	12-3189-41
			100 tests	12-3189-42
		Alexa Fluor 647	25 tests	51-3189-41
			100 tests	51-3189-42
CD321 (F11R)	CSTEM27	Unconjugated	25 µg	14-3219-80
			100 µg	14-3219-82
		PE	25 tests	12-3219-41
			100 tests	12-3219-42
		Alexa Fluor 488	25 tests	53-3219-41
			100 tests	53-3219-42
Desmoglein 2 (DSG2)	CSTEM28	Unconjugated	25 µg	14-9159-80
			100 µg	14-9159-82
		PE	25 tests	12-9159-41
			100 tests	12-9159-42
		Alexa Fluor 488	25 µg	53-9159-80
			100 µg	53-9159-82
P-cadherin (CDH3)	CSTEM29	Unconjugated	25 µg	14-2237-80
			100 µg	14-2237-82
		APC	25 tests	17-2237-41
			100 tests	17-2237-42

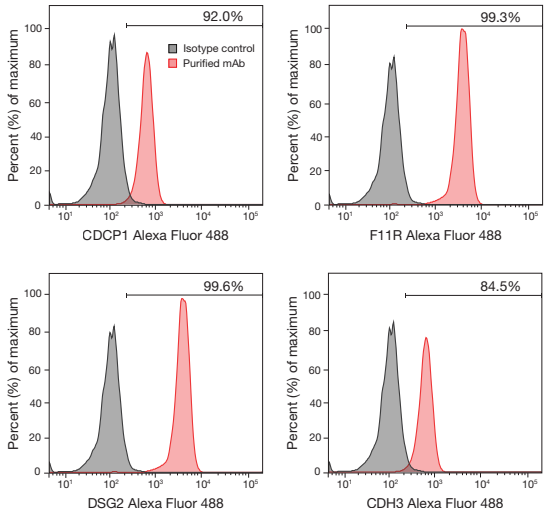

Figure 2. Immunostaining of undifferentiated human pluripotent stem cells using stem cell–specific cell-surface markers. Live undifferentiated WA09 human embryonic stem cells (hESCs) were immunolabeled with anti-CDCP1, anti-F11R, anti-DSG2, anti-CDH3 monoclonal antibodies (pink peak) or the corresponding isotype control (gray peak), detected with Invitrogen™ Alexa Fluor™ 488 secondary antibodies, and analyzed by flow cytometry. The histograms show that a high percentage of total live WA09 hESCs express the stem cell–specific antigens.

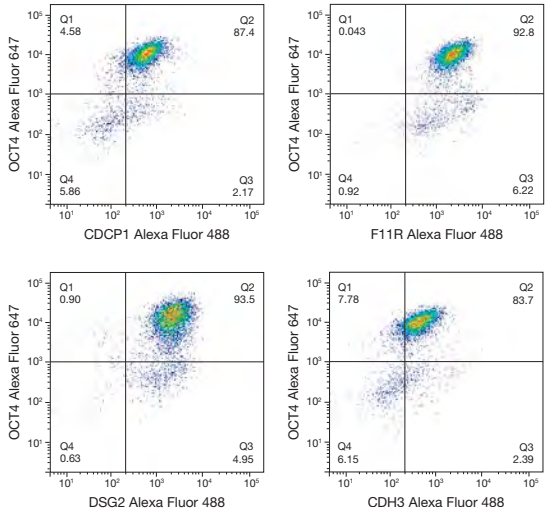

Figure 3. Coexpression of stem cell–specific cell-surface proteins and the transcription factor OCT4 on human embryonic stem cells. Flow cytometry dot plots show high coexpression of human pluripotent stem cell (hPSC)–specific cell-surface proteins (detected with CSTEM clones and Invitrogen™ Alexa Fluor™ 488 secondary antibodies) and OCT4 (detected with anti-OCT4 antibody and Invitrogen™ Alexa Fluor™ 647 secondary antibody) following sequential live- and fixed-cell immunolabeling of WA09 human embryonic stem cells (hESCs).

References

1. Laslett AL, Filipczyk AA, Pera MF (2003) *Trends Cardiovasc Med* 13:295–301.
2. O'Brien CM, Chy HS, Zhou Q et al. (2017) *Stem Cells* 35:626–640.
3. Kolle G, Ho M, Zhou Q et al. (2009) *Stem Cells* 27:2446–2456.

The new generation of target-specific protein quantitation

Introducing ProQuantum high-sensitivity immunoassays.

Many tools and strategies have been developed to advance our understanding of human diseases and their cellular mechanisms, as well as to design more effective screening, prevention, and treatment methods. However, a simple, scalable, and affordable process for validating biomarkers or measuring extremely low levels of analytes in limited, hard-to-obtain samples has seemed out of reach. Our latest platform innovation—Invitrogen™ ProQuantum™ high-sensitivity immunoassays—is a set of ready-to-use kits for quantifying low-abundance proteins in small sample volumes (as little as 2–5 µL of serum). These high-performance singleplex immunoassays run on any qPCR instrument and typically require 2 hours from sample to answer.

ProQuantum immunoassays: How they work

ProQuantum immunoassays work by leveraging proximity ligation assay (PLA™) technology. The combination of powerful proteomic tools, including high-specificity antibody–antigen binding and Invitrogen™ SiteClick™ antibody labeling, with genomic tools such as Applied Biosystems™ TaqMan® qPCR technology produces a detection method with both high sensitivity and a broad dynamic range (Figure 1). With a fast and easy workflow and very small sample consumption requirements, the ProQuantum immunoassay platform can detect much lower levels of protein analyte than traditional methods (Figure 2). Moreover, these immunoassays can quantify analytes over a concentration range of 5 orders of magnitude or more, minimizing the need for sample dilutions.

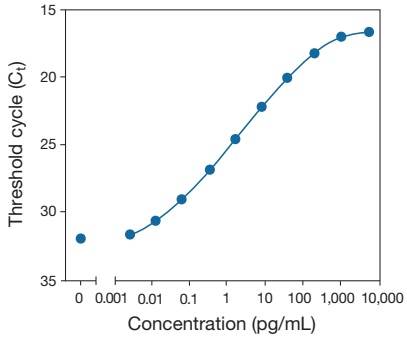

Figure 1. A 10-point standard curve for the ProQuantum human IL-8 immunoassay, demonstrating the assay's large dynamic range and sensitivity at extremely low target-protein concentrations. The IL-8 recombinant protein provided in the Invitrogen™ ProQuantum™ Human IL-8 Immunoassay Kit (Cat. No. A35575) was serially diluted 5-fold from a starting concentration of 5,000 pg/mL to 0.00256 pg/mL and then amplified according to the assay protocol to generate a standard curve that spans over 5 logarithmic units and shows low-end separation for quantitation of small amounts of protein. See Figure 3 for more details on the assay.

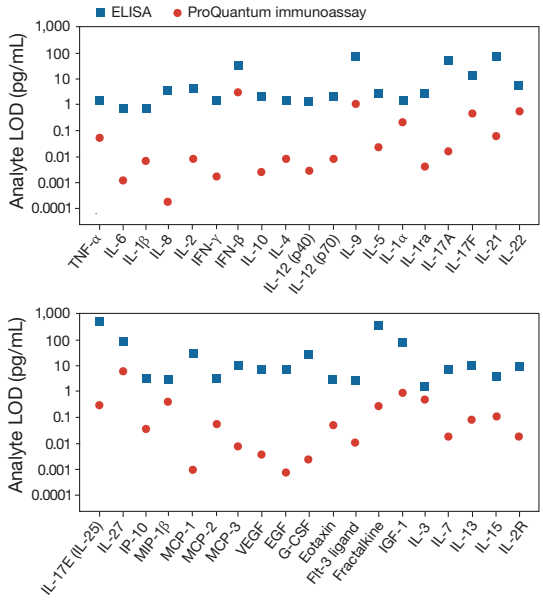

Figure 2. Analytical sensitivity comparison between ProQuantum and ELISA platforms. As compared with ELISAs, ProQuantum immunoassays show lower limit-of-detection (LOD) values for the same protein target. On average, ProQuantum immunoassays are 10- to 100-fold more sensitive than ELISAs.

The assay is based on target-specific antibodies that are methodically screened to develop an optimized pair of antibodies that bind to epitopes in close proximity on an antigen. These antibodies are preconjugated to DNA oligonucleotides at either the 3′ end (60 bases) or the 5′ end (40 bases) of the nucleic acid (Figure 3A). When the two antibodies are added to a sample suspension containing the specific protein to be quantitated, the two antibodies bind to their respective binding sites on the antigen, which results in the two oligonucleotide strands being brought in proximity (Figure 3A). This antibody binding provides structural stability such that in the presence of DNA ligase and a third oligonucleotide connector (complementary to the ends of each of the original two DNA oligonucleotides), the two antibody-conjugated oligonucleotides are ligated together to create a 100-base strand that can serve as a DNA amplification template (Figure 3B). Following a temperature increase to 95°C to inactivate the ligase and denature the analyte proteins and antibodies, the DNA templates are amplified through

40 cycles of TaqMan fluorescence-based qPCR. The amount of DNA produced is measured after each amplification cycle via the fluorescence increase, which is directly proportional to the number of PCR product molecules (or amplicons) generated.

Analysis of ProQuantum data

Figure 3 shows the ProQuantum immunoassay workflow and data produced. The fluorescence produced during amplification of the DNA template is measured throughout the qPCR cycling and plotted against the cycle number (Figure 3C). With high concentrations of protein analyte in the sample, a lower cycle number is needed to reach a given fluorescence threshold (threshold cycle or C_t); conversely, with lower protein concentrations, a higher cycle number is required. Analyte concentration values can be interpolated from a dose-response curve, generated using known protein concentrations (Figure 3D).

To facilitate quantitative measurements, we have developed intuitive, user-friendly, cloud-enabled software to provide easy standard curve fitting and analysis, including statistical groupwise comparison. The ProQuantum immunoassay is extremely sensitive, enabling quantitation of basal cytokine levels in normal human serum (Figure 4), as well as in other research model systems in which there is a need to interrogate low-abundance proteins.

A ProQuantum assay for your target

The ProQuantum immunoassay platform and software provide a simple yet sophisticated solution for quantitative immunoassays, with a typical sample-to-answer time of 2 hours. See the most up-to-date list of target proteins and learn more about ProQuantum immunoassays at **thermofisher.com/proquantumbp76**. ■

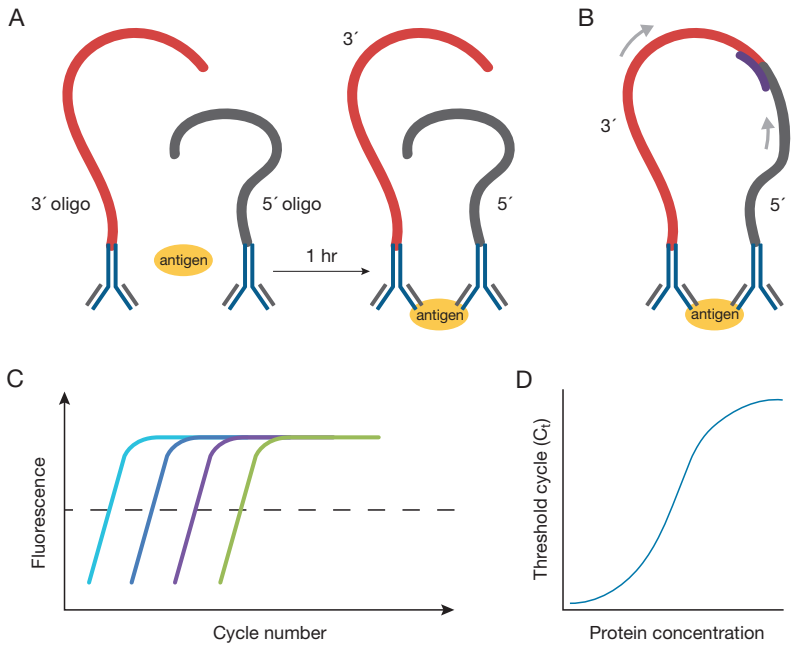

Figure 3. How ProQuantum immunoasssays work. (A) Antibody–antigen binding: Antibodies bind to two separate epitopes on the antigen (during a 1 hr incubation), which brings the two conjugated oligonucleotides into close proximity. **(B)** Ligation and amplification of signal (in a qPCR instrument): DNA ligase and a third oligonucleotide connector are added to ligate the two ends of the conjugated oligonucleotides, creating a 100-base DNA template. Once the ligase is inactivated at 95°C, the sample is amplified through 40 cycles of annealing and extension. **(C)** The amount of DNA produced is measured after each amplification cycle via fluorescent dyes, which exhibit fluorescence that is directly proportional to the number of PCR product molecules (or amplicons) generated. This graph shows the fluorescence vs. cycle number curves for four different starting protein concentrations. The dashed line represents the fluorescence threshold. **(D)** The cycle number required to reach the fluorescence threshold (threshold cycle or C_t) is plotted vs. protein concentration to create a standard curve.

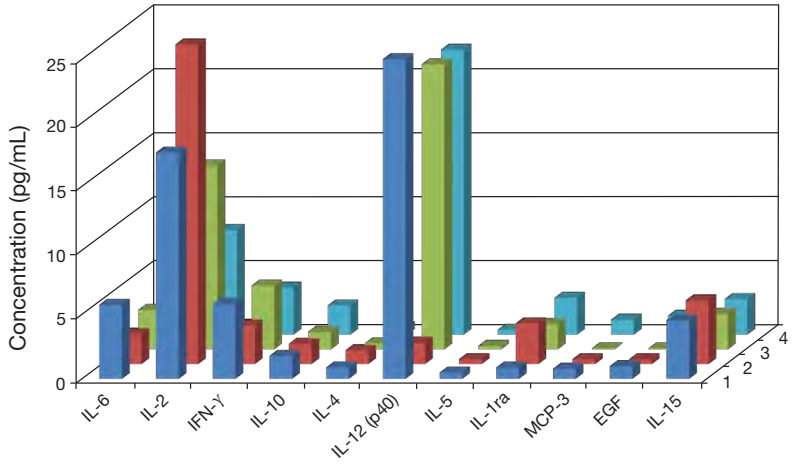

Figure 4. Sensitive cytokine detection in human serum using ProQuantum immunoassays. Sera from four healthy donors (labeled 1 through 4 on the z axis) were assayed with 11 different Invitrogen™ ProQuantum™ immunoassay kits to demonstrate the sensitivity of the assays. These low pg/mL concentrations were interpolated from standard curves generated for each target; none of the values fell outside of the lowest point on the standard curve.

Stunningly easy western blot imaging

Introducing the iBright CL1000 and iBright FL1000 Imaging Systems.

Despite the rapid pace of technological advances in life science research, nucleic acid gels, protein gels, and western blots continue to be fundamental laboratory tools with the ability to move a project forward or push it in a whole new direction. The Invitrogen™ iBright™ Imaging Systems are high-performance instruments for capturing images and analyzing data from gels and blots. Designed with a streamlined intuitive interface and advanced automated features, the iBright systems are easy to use for researchers at all experience levels.

Figure 1. The iBright FL1000 Imaging System.

iBright CL1000 and iBright FL1000 Imaging Systems

Two iBright instruments are available: the iBright CL1000 system, for imaging and documenting chemiluminescent western blots and colorimetrically stained protein and nucleic acid gels, and the iBright FL1000 system (Figure 1), which features the same imaging modes as the iBright CL1000 system but also offers fluorescent gel and blot imaging capability using visible and near-IR excitation and emission channels (Table 1).

Advantages of the iBright Imaging Systems

- Powerful 9.1 megapixel cooled 16-bit CCD camera—for capturing crystal-clear images with robust imaging potential (Figure 2).
- Push-button optimized exposure with Invitrogen™ Smart Exposure™ technology—for rapid determination of optimal exposure times, minimizing the need to repeat exposures to get the desired signal.
- Advanced automated features—allowing hassle-free sample alignment, focus, and zoom, as well as automatic on-board data analysis for instantaneous lane and band identification and molecular weight marker overlay.
- Long-life green LED-based transilluminator—providing a light source that can effectively excite popular DNA dyes (e.g., ethidium bromide and Invitrogen™ SYBR™ Green dyes), without exposing users to harmful UV radiation.
- Cloud connectivity with Invitrogen™ iBright™ Analysis Software—enabling export and storage of data, as well as the ability to access, review, analyze, and share data through the web-based Thermo Fisher Cloud platform.
- Extensive service and support—from the on-site Invitrogen™ SmartStart™ orientation (included with every system) to our highly responsive technical and field support teams and comprehensive post-warranty service plans.

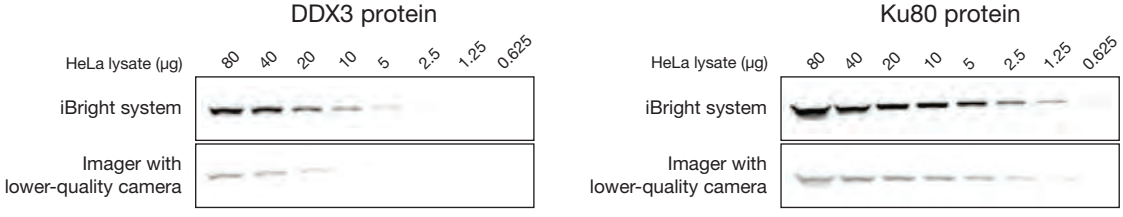

Figure 2. iBright Imaging Systems feature a powerful 9.1 megapixel camera for sensitive signal detection. Two-fold serial dilutions of HeLa cell lysate (starting at 80 µg/lane) were loaded and run on Invitrogen™ Novex™ Tris-glycine gels, transferred, and probed with antibodies against DDX3 or Ku80 protein. Blots were then probed with corresponding HRP-conjugated secondary antibodies, developed with Thermo Scientific™ SuperSignal™ West Pico PLUS Chemiluminescent Substrate (Cat. No. 34577), and visualized (using 10 sec exposures) on either the Invitrogen™ iBright™ FL1000 Imaging System or another imaging device with a lower-quality, 4.1 megapixel camera.

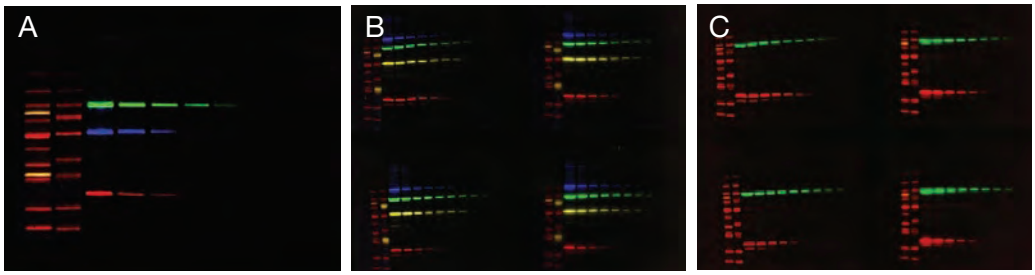

Figure 3. Multiplexed fluorescence western blots visualized using the iBright FL1000 Imaging System. (A) 3-color blot. **(B)** 4-color high-throughput image with 4 mini blots. **(C)** 2-color high-throughput image with 4 mini blots. Experimental details are available at **thermofisher.com/ibright**.

iBright FL1000 system for fluorescence applications

The iBright FL1000 Imaging System employs the same green LED-based transilluminator as the iBright CL1000 Imaging System, as well as two high-quality long-life epi-LEDs for fluorescence imaging applications. The broad-spectrum white epi-LED can be used to excite most green-, red-, and far-red–fluorescent dyes, including antibody conjugates labeled with Invitrogen™ Alexa Fluor™ and Alexa Fluor™ Plus dyes, Thermo Scientific™ DyLight™ dyes, and Invitrogen™ WesternDot™ dyes. The second epi-LED emits longer-wavelength light and is optimized for near-IR fluorophores such as Alexa Fluor 790 and Alexa Fluor Plus 800 dyes, DyLight 800 dye, and WesternDot 800 dye.

Light from these LED sources, in conjunction with both excitation and emission filters, enables many possible reagent options for nucleic acid gel, protein gel, and western blot imaging applications. The iBright FL1000 model features five fluorescence channels, three in the visible fluorescence range and two in the near-IR fluorescence range (Table 2). Up to four channels can be multiplexed simultaneously when imaging a single western blot or set of four mini blots (Figure 3). Multiplex western blotting allows the study of multiple proteins in a single blot, while also providing more accurate comparisons of experimental data and controls. Smart Exposure technology further improves acquisition of multiplex fluorescence western blot data because its advanced auto-exposure functionality can help to optimize signal-to-noise ratios for each fluorescence channel separately.

Product	Quantity	Cat. No.
iBright™ CL1000 Imaging System	1 system	A32749
iBright™ FL1000 Imaging System	1 system	A32752
iBright™ Prestained Protein Ladder	2 x 250 µL	LC5615

See the iBright Imaging Systems for yourself

To learn more about the iBright FL1000 and iBright CL1000 Imaging Systems and request an in-lab demonstration, visit **thermofisher.com/ibrightbp76**. There you can download the iBright Imaging Systems brochure, which shows a variety of data acquired and analyzed using the iBright systems, a list of dyes and stains compatible with the iBright imaging modes, and complete instrument specifications. Find out how these high-performance instruments can enhance gel and western blot analysis in your laboratory. ■

Table 1. Imaging modes of the iBright FL1000 and iBright CL1000 systems.

Imaging capability	What kind of signal can be captured?
Protein gel	Colorimetric staining of gels (e.g., Coomassie and silver stains) and membranes (e.g., Ponceau S and MemCode stains)
Nucleic acid gel	Ethidium bromide and SYBR dye staining
Chemiluminescent blot	Chemiluminescence detection using all popular horseradish peroxidase (HRP) and alkaline phosphatase (AP) substrates (e.g., SuperSignal and WesternBreeze substrates)
Fluorescent blot*	Fluorescence detection using RGB (visible range) and near-IR fluorophores (e.g., Alexa Fluor and Alexa Fluor Plus dyes and DyLight dyes)

*iBright FL1000 Imaging System only.

Table 2. Filter sets on the iBright FL100 Imaging System.

Excitation	Filter (nm)	Emission	Filter (nm)	Example of a compatible Alexa Fluor Plus dye
EX1	455–485	EM1	510–555	Alexa Fluor Plus 488
EX2	515–545	EM2	565–615	Alexa Fluor Plus 555
EX3	610–635	EM3	675–720	Alexa Fluor Plus 647
EX4	655–680	EM4	725–750	Alexa Fluor Plus 680
EX5	745–765	EM5	810–850	Alexa Fluor Plus 800

Optimize protein integrity and yields during workflows

Broad-spectrum protease and phosphatase inhibitor tablets.

Inside a cell, proteins are commonly separated from proteolytic enzymes through differential localization. Disruption of cellular and tissue architecture during protein extraction distorts the *in vivo* state by making all proteins potentially accessible for degradation or modification by endogenous proteases and phosphatases. Unregulated, these activities can reduce protein yield and function in a sample. To minimize these losses, protease and phosphatase inhibitors can be added during cell lysis to prevent degradation of extracted proteins and preserve protein structure, function, and yields during sample preparation.

Protease and phosphatase inhibitors

Protease and phosphatase inhibitor cocktails and tablets are ideal for protecting proteins during extraction procedures or lysate preparation using primary cells, cultured mammalian cells, animal tissues, plant tissues, yeast cells, or bacterial cells. Formulations are packaged in multiple sizes, and EDTA-free versions are available for divalent cation–sensitive assays. Thermo Scientific™ Pierce™ inhibitor mini tablets have been reformulated to dissolve quickly into a clear solution and are fully compatible with all Pierce protein assays. Figures 1 and 2 provide representative examples of the effectiveness of Pierce Protease and Phosphatase Inhibitor Mini Tablets.

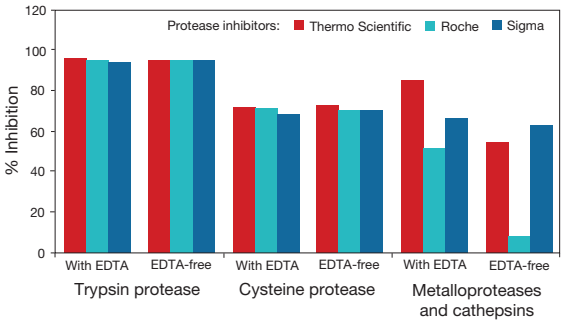

Figure 1. Performance comparison between three commercially available protease inhibitor tablets. Pancreatic extract (100 µL, 0.5 µg/µL) was incubated with cleavable fluorogenic substrates for trypsin and cysteine proteases, metalloproteases, and cathepsins in the presence of Thermo Scientific™ Pierce™ Protease Inhibitor Mini Tablets (Cat. No. A32953), Roche cOmplete™ Protease Inhibitor Tablets, and Sigma-Aldrich SIGMAFAST™ Protease Inhibitor Cocktail Tablets, with and without EDTA. Reactions were incubated for 1 hr at 37ºC, and fluorescence was determined at the appropriate detection emission wavelengths on a Thermo Scientific™ Varioskan™ Flash microplate reader. Percent protease inhibition is shown for each protease inhibitor formulation.

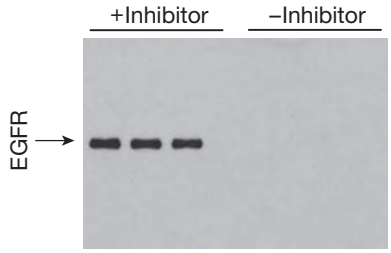

Figure 2. Inhibition of phosphatase activity in human colorectal carcinoma cell lysate. HCT116 cells were serum-starved and treated with epidermal growth factor (EGF) for 15 min or left untreated as controls (data not shown). Cell lysates were prepared in Thermo Scientific™ Pierce™ IP Lysis Buffer (Cat. No. 87788) with or without Thermo Scientific™ Pierce™ Protease and Phosphatase Inhibitor Mini Tablets, EDTA-Free (Cat. No. A32961) and incubated with anti–phosphotyrosine antibody overnight at 4ºC. The immunoprecipitated complex was incubated with Thermo Scientific™ Pierce™ Protein A/G Magnetic Beads (Cat. No. 88803) for 1 hr at room temperature. After washing the beads, a low-pH elution was performed, and this eluate was run on a gel, transferred to a membrane, and probed with anti–EGF receptor (EGFR) antibody prior to chemiluminescence western blot detection.

Download the free Protein Preparation Handbook

The Protein Preparation Handbook provides technical information on our broad portfolio of reagents and tools for protein extraction, cleanup, immunoprecipitation, and purification, including the inhibitor tablets discussed here. Practical information, selection guides, and relevant data are included to help improve protein yield, facilitate downstream analysis, and optimize workflows. Download this free brochure at **thermofisher.com/proteinprephandbook**. We have also produced a series of self-paced animated eLearning modules—including a free course on protein sample preparation—which can be accessed at **thermofisher.com/elearningcourses**. ■

Product	Quantity	Cat. No.
Pierce™ IP Lysis Buffer	100 mL 250 mL	87787 87788
Pierce™ Protease Inhibitor Mini Tablets	30 tablets	A32953
Pierce™ Protease Inhibitor Tablets	20 tablets	A32963
Pierce™ Protease Inhibitor Mini Tablets, EDTA-free	30 tablets	A32955
Pierce™ Protease Inhibitor Tablets, EDTA-free	20 tablets	A32965
Pierce™ Phosphatase Inhibitor Mini Tablets	20 tablets	A32957
Pierce™ Protease and Phosphatase Inhibitor Mini Tablets	20 tablets	A32959
Pierce™ Protease and Phosphatase Inhibitor Mini Tablets, EDTA-free	20 tablets	A32961

Behind the bench: What are event rates and should you always trust the "Maximum Event Rate" of your flow cytometer?

Greg Kaduchak, Principal Engineer, Thermo Fisher Scientific.

What is the "event rate"?

In flow cytometry, an "event" is defined as a single particle detected by the instrument. Accurate detection of events using flow cytometry requires the ability to separate single cells with specific characteristics from within a heterogeneous population of cells. Detection can be complicated by the challenge of detecting the cells of interest in a limited sample or in the presence of cell debris or other artifacts of sample preparation.

When investigating a population of cells, it may be necessary to acquire 10^4 to 10^7 events to obtain a sufficient number of cells for statistically significant detection. The number of events needed for analysis depends on three main factors: the ratio of cells to debris in the sample, the signal-to-noise ratio of the detected cells compared to background fluorescence, and the frequency of the cell population of interest in the sample. Poisson statistics apply when counting randomly distributed populations, where precision increases as more events are acquired [1]. To determine the size of the sample (number of cells) that will provide a given precision, the equation $r = (100/CV)^2$ is used, where r is the number of cells meeting the defined criterion of the rare event, and CV is the coefficient of variation of a known positive control.

How are event rates calculated and how does this vary between instruments?

I have recently received a number of questions related to the calculation of the Maximum Event Rate of a flow cytometry instrument. Much of the conversation has been directed toward how the Maximum Event Rate, as calculated by different methods, may affect instrument performance.

There are several methods by which Maximum Event Rate of a flow cytometer is calculated. A standard, more accurate method is to define the Maximum Event Rate as the analysis rate where 10% of all events are coincident (according to Poisson statistics). For this method, the coincidence rate is one of the foundational values in the flow cytometer design. This is our method of design for the Invitrogen™ Attune™ NxT Flow Cytometer.

Another method is to cite the Maximum Event Rate of the electronic data collection system. This method has become more popular with some manufacturers in recent years due to the advent of fast and less expensive electronic circuitry. A system designed with this method is agnostic to coincidence and thus can result in a very high rate of coincidence at the instrument's specified Maximum Event Rate.

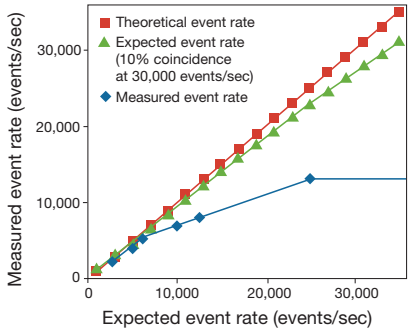

Figure 1. Plot of measured event rate vs. expected event rate on a flow cytometer. The theoretical event rate (red) assumes no coincidence between events. The expected event rate (green) assumes 10% of all events are coincident, according to Poisson statistics, and is the method used in the design of the Invitrogen™ Attune™ NxT Flow Cytometer. The measured event rate (blue) shows the data from an instrument review conducted by the University of Chicago core facility (**ucflow.blogspot.com/2014/09/a-first-look-at-beckman-coulter.html**).

Calculation of Maximum Event Rates

- Standard method: Analysis rate where 10% of all events are coincident (according to Poisson statistics).
- Alternative method: Cite the Maximum Event Rate of the electronic data collection system.

Why is coincidence so important in a flow cytometer's design?

Simply put, coincident events are indeterminate and do not possess valuable information. Worse, coincidence injects "polluted" events into the experiment. Researchers attempt to gate coincident events out of their experiment by using bivariate plots with combinations of height, width, and area data, but unfortunately there is no method to fully remove them. Thus, to keep the data integrity as high as possible, it is best to keep coincident events to a minimum. In addition, it affects absolute counts, as events that contain two or more particles count only as one particle. →

How does calculated Maximum Event Rate differ?

Let's look at an example of how coincidence events enter the data as a function of analysis rate. Consider an instrument designed using the 10% coincidence method with a specified Maximum Event Rate of 30,000 events/sec. The plot in Figure 1 shows the theoretical event rate when no events are coincident. It also shows the expected event rate, which is the analysis rate that is measured when allowing 10% coincidence. As seen, the expected event rate is lower than the theoretical event rate since coincident events count only as a single event. At 30,000 events/sec, one can see there is a 10% difference in the event rates (by design). Note that coincidence increases as a function of analysis rate.

Next, compare the theoretical and expected event rate data with the data from an instrument review conducted by researchers at the University of Chicago (**ucflow.blogspot.com/2014/09/a-first-look-at-beckman-coulter.html**). The measured event rate on this instrument (Figure 1) deviates greatly from the expected event rate calculated by the 10% coincidence method as opposed to the maximum speed of the electronics. As can be seen, not only does the measured event rate deviate, it never attains an analysis rate greater than approximately 14,000 events/sec.

Why such a large difference? It could be that the instrument's electronic system cannot process events at rates greater than 14,000 events/sec. If this is the case, then 30,000 events/sec is not attainable whether events are coincident or not.

It is also possible that the instrument reaches such a high rate of coincidence that most events are coincident and counted as doublets, triplets, etc. For this assumption, let's consider a cytometer designed for a Maximum Event Rate of 4,500 events/sec as calculated by the 10% coincidence method (Figure 2). The data look strikingly similar to the measured test data. So, if the instrument's Maximum Event Rate is calculated using the standard method and the same one used for the Attune NxT Flow Cytometer, the Maximum Event Rate of this instrument would be 4,500 events/sec, not 30,000 events/sec. At 30,000 events/sec, coincident events occur at a rate of approximately 15,000 events/sec.

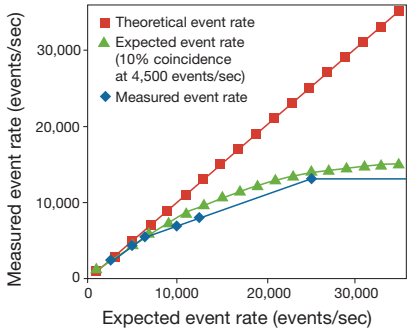

Figure 2. Plot of measured event rate vs. expected event rate. The theoretical event rate (red) assumes no coincidence between events. In this expected event rate (green), we assume 10% coincidence for a Maximum Event Rate of 4,500 events/sec in order to better predict the measured event rate. The measured event rate (blue) shows the data from an instrument review conducted by the University of Chicago core facility (**ucflow.blogspot.com/2014/09/a-first-look-at-beckman-coulter.html**).

It is important that flow cytometrists understand these differences and how it can affect their research. In an upcoming post on our blog, we will look at how a system can attain such high coincidence rates. Interestingly, it does not have anything to do with how much time the particles spend in the laser, but we will leave that discussion for another post. Visit **thermofisher.com/flowblog** for more posts from flow cytometry researchers. ■

Reference

1. Hedley BD, Keeney M (2013) *Int J Lab Hematol* 35:344–350.

Behind the Bench blog goes with the flow

Do you use a flow cytometer? Ever wonder about the true definition of an event rate and if you should trust the "maximum event rate" of your flow cytometer (see above)? Want to delve into flow cytometry fluidics or learn about the newest family of antibody conjugates for flow cytometry—the Invitrogen™ eBioscience™ Super Bright antibody conjugates? Visit the Behind the Bench blog by Thermo Fisher Scientific to hear directly from researchers in the field. Read all about it at **thermofisher.com/flowblog**.

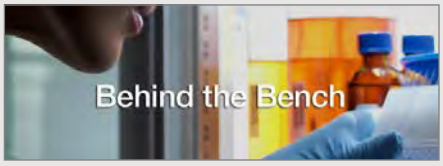

Time-resolved analysis of proteome dynamics by tandem mass tags and stable isotope labeling in cell culture (TMT-SILAC) hyperplexing

Welle KA, Zhang T, Hryhorenko JR, Shen S, Qu J, Ghaemmaghami S (2016) *Mol Cell Proteomics* 15:3551–3563.

The protein composition of a cell at any given time defines the cell's health and function. A specific protein's abundance, localization, and lifetime has traditionally been studied with antibodies or other highly selective tags. In order to conduct a global analysis of protein dynamics, Welle and coworkers recently described a method that employs metabolic isotopic labeling (stable isotope labeling in cell culture or SILAC) in combination with isobaric tagging for the multiplexed mass spectrometry analysis of complex protein samples at different time points.

In recent years, the field of mass spectrometry has exploded with advances in both instrumentation and methodology that allow quantitative analysis of complex mixtures. Tandem mass spectrometry (LC-MS/MS) provides a means of defining the composition, expression levels, and modifications of proteins in a given sample at a precise time point. This proteome snapshot, however, cannot capture the dynamics of protein expression, including the kinetics of protein synthesis and clearance and the ongoing modifications of proteins that define their function.

Welle and coworkers have addressed the limitations inherent in a static proteome analysis by combining dynamic SILAC experiments with isobaric tagging to produce highly multiplexed (i.e., hyperplexed) samples that can be analyzed in a single mass spectrometry run. SILAC is a standard protocol for metabolically incorporating $^{15}N/^{13}C$-labeled amino acids into proteins and then analyzing these isotope labels using LC-MS/MS. Dynamic SILAC further integrates a time component into the labeling—either by pulsing the labeled amino acids in cell culture media or by sampling the cells over time—to allow proteome-wide determination of protein synthesis and degradation kinetics. In the method reported here, samples acquired at each time point were labeled with a unique isobaric tag (tandem mass tag or TMT) before combining them into a single hyperplexed sample for analysis by LC-MS/MS.

To determine the effectiveness of this method, these researchers used the combination of SILAC and TMT labeling with LC-MS/MS analysis to measure the kinetics of protein turnover for over 3,000 proteins in human dermal fibroblasts and compared the results with those obtained using non-multiplexed methods. They obtained similar rates for protein synthesis and degradation when time points were analyzed with either TMT-SILAC hyperplexing within a single mass spectrometry run or dynamic SILAC across multiple mass spectrometry runs.

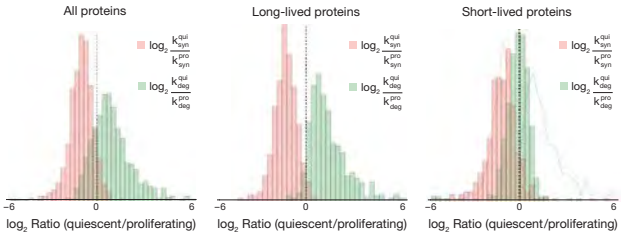

Figure 1. The use of TMT-SILAC hyperplexing to measure relative differences in synthesis rates (k_{syn}) and degradation rates (k_{deg}) between quiescent and proliferating cells. Histograms of the distribution of $\log_2$ ratios of k_{syn} and k_{deg} between quiescent and dividing cells are shown for all proteins, long-lived proteins (half-lives >3 days in proliferating cells) and short-lived proteins (half-lives <3 days in proliferating cells). The dotted lines on the rightmost plot indicate the distribution of long-lived proteins for comparison. Reprinted with permission from Welle KA, Zhang T, Hryhorenko JR et al. (2016) *Mol Cell Proteomics* 15:3551–3563.

Dynamic SILAC provided slightly better precision, but the TMT-SILAC hyperplexing method was improved by adding synchronous precursor selection (SPS) to minimize interference from co-isolated interfering ions.

Welle and coworkers then combined their TMT-SILAC samples acquired at different time points from both quiescent and proliferating fibroblasts into a single hyperplexed sample to simultaneously measure the ratios of synthesis and degradation rate constants in these two cell states (Figure 1). As expected, they found that protein synthesis was globally decreased in quiescent cells compared with that in proliferating cells, presumably to compensate for the lack of cellular growth. They also observed that protein degradation rates were increased in quiescent cells, particularly for long-lived proteins. They note that this study is the first quantitative global census of protein synthesis and protein degradation rates in quiescent cells. Their experiments demonstrate that the use of TMT-SILAC hyperplexing with a single LC-MS/MS run should simplify the time-resolved analysis of proteome dynamics in different cell environments or in reaction to different stimuli, while also reducing the time and costs associated with multiple mass spectrometry runs. ■

Product	Quantity	Cat. No.
MEM for SILAC	500 mL	88368
Pierce™ C18 Spin Tips	96 tips	84850
Pierce™ High pH Reversed-Phase Peptide Fractionation Kit	12 reactions	84868
Pierce™ Trypsin Protease, MS Grade	5 x 20 µg	90057
TMT10plex™ Isobaric Label Reagent Set	30 reactions	90111

An evaluation of spectrally distinct succinimidyl ester dyes for tracking cell proliferation by flow and image cytometry

McDonald D, Clarissa A, Bradford J, Meeson A, Filby A (2017) Poster presented at: CYTO 2017, 32nd Congress of the International Society for Advancement of Cytometry; July 10–14, 2017; Boston, Massachusetts, USA.

The study of cell proliferation has widespread applications in fields as diverse as embryogenesis, immunology, and cancer biology. In *BioProbes 73*, we highlighted the methods developed by Filby and coworkers to evaluate amine-reactive fluorogenic dyes used for tracking cell proliferation by flow and image cytometry [1–3]. At the CYTO 2017 meeting, they presented their work with two recently introduced amine-reactive dyes—the UV-excitable Invitrogen™ CellTrace™ Blue dye and the 532 nm– or 561 nm—excitable Invitrogen™ CellTrace™ Yellow dye. When used in conjunction with flow or image cytometry, fluorogenic succinimidyl ester (SE) dyes, such as the CellTrace proliferation dyes, provide a means of following the proliferative history of a single cell *in vivo* or *in vitro*.

The CellTrace proliferation dyes are designed to pass freely through cell membranes, where they are cleaved by intracellular esterases and spontaneously react with intracellular proteins through lysine side chains and other available amine groups, producing highly fluorescent, cell-impermeant proteins (see **thermofisher.com/celltrace**). These fluorescent proteins are distributed equally between daughter cells during cell division, such that each daughter cell exhibits half the fluorescence intensity of the parent cell, which is readily detectable by flow cytometry, fluorescence microscopy, or a fluorescence microplate reader. To be effective, dyes for tracking proliferation should: 1) exhibit intense and homogeneous fluorescent labeling of the parent cell that can be followed through successive cell divisions, 2) be available in a choice of excitation and emission wavelengths to facilitate multiparametric measurements and reduce compensation requirements, and 3) not perturb cell proliferation throughout the observation period.

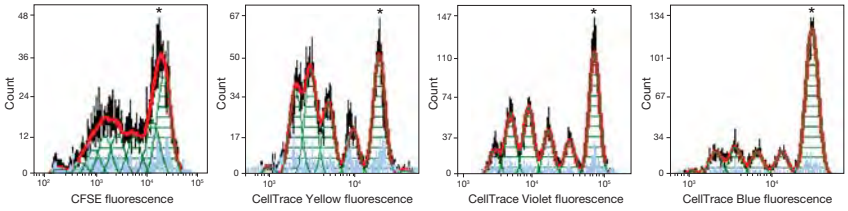

Figure 1. Data showing the proliferative performance of human peripheral blood mononuclear cells (PBMCs) stained with four different CellTrace proliferation dyes. *Peak corresponding to undivided cells. Reprinted with permission from Andrew Filby, Newcastle University, United Kingdom.

In their CYTO 2017 poster, McDonald and coworkers describe their flow cytometric evaluation of CellTrace proliferation dyes using either Jurkat cells or human peripheral blood mononuclear cells (PBMCs) activated with phytohemagglutinin (PHA) in the presence of interleukin-2 (IL-2); DAPI or propidium iodide staining was used to exclude dead cells. For each CellTrace dye and cell type, the dye was first titrated to find the optimal labeling concentration before conducting the cell proliferation analysis. For the Jurkat T cells and PBMCs, optimal concentrations of 8 µM were determined for CellTrace Blue and CellTrace Yellow dyes, and 4 µM for CellTrace Violet and CellTrace Far Red dyes. Labeled cells were then analyzed every 24 hours over a 96-hour period for percentage divided, proliferation index, and mean division metrics by flow cytometry (Figure 1). McDonald and coworkers confirmed earlier findings that CellTrace CFSE proliferation dye—the original fluorescein derivative—negatively affected cell proliferation and produced poor division peak quality and resolution, which hindered observation of successive generations. They conclude that, while all SE dyes are not equivalent in terms of proliferative performance, the CellTrace proliferation dyes, including the recent CellTrace Blue and CellTrace Yellow additions, provide useful and reliable tools for tracking cell division by flow and image cytometry. ■

References

1. Begum J, Day W, Henderson C et al. (2013) *Cytometry A* 83:1085–1095.
2. Filby A, Begum J, Jalal M et al. (2015) *Methods* 82:29–37.
3. *BioProbes 73 Journal of Cell Biology Applications* (May 2016) Journal Club: Appraising the suitability of succinimidyl and lipophilic fluorescent dyes to track proliferation in non-quiescent cells by dye dilution. **http://www.thermofisher.com/bp73**

Product	Laser for excitation	Ex/Em*	Quantity†	Cat. No.
CellTrace™ Blue Cell Proliferation Kit	UV	355 or 375/410	180 reactions	C34568
CellTrace™ Violet Cell Proliferation Kit	405 nm	405/450	180 reactions	C34557
CellTrace™ CFSE Cell Proliferation Kit	488 nm	495/519	180 reactions	C34554
CellTrace™ Yellow Cell Proliferation Kit	532, 561 nm	546/579	180 reactions	C34567
CellTrace™ Far Red Cell Proliferation Kit	633, 635 nm	630/661	180 reactions	C34564

*Excitation (Ex) and emission (Em) maxima in nm, after hydrolysis. †CellTrace kits are also available for 20 reactions.

Cover image

Visualizing a mouse cortical neuron culture. Cryopreserved Gibco™ Primary Mouse Cortical Neurons (Cat. No. A15585) were grown in culture for 3 weeks using the Gibco™ B-27™ Plus Neuronal Culture System (Cat. No. A3653401). Cells were fixed and labeled with Invitrogen™ NucBlue™ Fixed Cell ReadyProbes™ Reagent (Cat. No. R37606), anti–β-3 tubulin mouse monoclonal antibody (Cat. No. 32-2600) in conjunction with Invitrogen™ Alexa Fluor™ 488 goat anti–mouse IgG antibody (Cat. No. A11029), and Invitrogen™ ActinRed™ 555 ReadyProbes™ Reagent (Cat. No. R37112). Cells were mounted in Invitrogen™ ProLong™ Glass Hard-Set Antifade Mountant (Cat. No. P36980) and imaged on an Invitrogen™ EVOS™ FL Auto 2 Imaging System using a 60x oil-immersion objective. For more information on the B-27 Plus Neuronal Culture System, see “Maximize survival of neurons derived from primary and stem cells” on page 22.

Previous issues

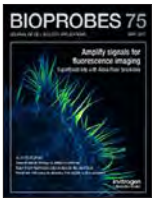

BIOPROBES 75

In this issue, we describe SuperBoost™ Kits with Alexa Fluor™ tyramides for signal amplification, as well as immune checkpoint antibodies, Super Bright antibody conjugates for the violet laser, and the PrimeFlow™ RNA assay for detecting RNA targets by flow cytometry. A center insert includes a fluorophore and reagent selection guide for flow cytometry.

BIOPROBES 74

This issue focuses on CRISPR-Cas9–based research, including the combination of genome editing and functional proteomics, as well as a description of our comprehensive portfolio of reagents for Cas9 delivery through cell function assays. Also highlighted are several stem cell studies and fluorescent reagents for flow cytometry and imaging, such as the FluxOR™ II Green K^+ channel assay.

BIOPROBES 73

This issue features Click-iT™ EdU and TUNEL colorimetric assays for immunohistochemistry, as well as Superclonal™ recombinant secondary antibodies. Also discussed are high-speed cell counting and generational tracing assays by flow cytometry, the TurboLuc™ Luciferase One-Step Glow Assay, and the SureCast™ Handcast and Novex™ WedgeWell™ precast protein gel systems.

Back issues of *BioProbes Journal* published after 1995 are available at **thermofisher.com/bioprobes**. Subscribe to *BioProbes Journal* at **thermofisher.com/subscribebp**.

Thermo Fisher Scientific
5781 Van Allen Way
Carlsbad, California 92008
United States
Tel: +1 760 603 7200
Toll-Free Tel: 800 955 6288
Fax: +1 760 603 7229
Email: techsupport@thermofisher.com

2014 APEX® AWARDS FOR PUBLICATION EXCELLENCE

For Research Use Only. Not for use in diagnostic procedures.

COL05116 1117

thermofisher.com/bioprobes

ThermoFisher SCIENTIFIC